

Evaluation of Hedging Strategies of Asian Options on Electricity at Nord Pool

Ella Zackrisson

June 1, 2015

Abstract

This thesis empirically evaluates a geometric Brownian motion and a stochastic volatility model for modeling futures prices and hedging Asian call options on the electricity spot price. Estimation of parameters for the models is done based on historical futures prices of futures contracts with a one month delivery period using nonlinear regression and Maximum Likelihood techniques. The models are tested on 2014 data and tracking error for each model is presented. The tracking error is investigated through the median value, the spread between minimum and maximum value along with value at risk at a 95% level.

In addition, a third model for modeling spot and futures prices is presented theoretically. It is an exponential additive model with the advantage that it models the future price process from the spot price, instead of modeling the future price process immediately. This bypasses the issue of no information about the future price process during the delivery period, when there is no prices of the futures contracts.

The aim of this thesis is to compare the simpler geometric Brownian motion to the more complex stochastic volatility model. It is found that the stochastic volatility model performs better when tested on out-of-sample data. The geometric Brownian motion tends to underestimate the electricity prices, despite that 2014 had low prices compared to the other years in the data sample. In addition, the approximation of the distribution of the future price process under the geometric Brownian motion model gave a bad fit and led to difficulties when estimating the parameters. The stochastic volatility model produced more stable results and gave a better fit for the distribution.

Keywords: Hedging strategies, Asian Options, Electricity

Acknowledgements

I would like to thank my supervisor at KTH Camilla Johansson Landén, my supervisor at SEB Cecilia Wingren and all the others in the Commodity-team for their support.

Stockholm, May 2015

Ella Zackrisson

Contents

1	Introduction	1
1.1	Dynamics of electricity spot price	1
1.2	Dynamics of electricity derivatives	3
1.3	Lévy processes	5
1.4	Problem formulation	7
2	Theory	9
2.1	Assumptions and definitions	9
2.2	Geometric Brownian motion	11
2.3	Stochastic volatility	14
2.4	Exponential additive process	21
2.5	Evaluation of models	26
3	Simulation of electricity futures prices	28
3.1	Data analysis	28
3.2	Geometric Brownian motion	29
3.3	Stochastic volatility	34
4	Results	40
4.1	Hedging error	40
4.2	Tracking error	43
5	Conclusion	45

Chapter 1

Introduction

The Asian style option was formerly traded at Nord Pool, but is now only provided OTC (over the counter) by financial institutions. The Asian option is a useful hedging instrument for industries when hedging the exposure to electricity in their production.

1.1 Dynamics of electricity spot price

Hedging options is closely related to pricing options and the behavior of the spot price. The behavior of the electricity spot price has several distinct characteristics that distinguish it from that of both stocks and other commodities. The spot electricity market is a day-ahead market, since the system operator must be able to check before the delivery if the required amount lies within transmission constraints (Weron, 2008). Typically the electricity spot price is an hourly contract with physical delivery (Weron et al., 2004).

Non-storability of electricity makes the electricity market different from other commodity markets. Shortages in electricity production or sudden increases in electricity demands result in peaks and jumps in the electricity spot price. The non-storability of electricity, not even for short periods of time, forces electricity to be generated and consumed instantaneously. Cash flows from generation and consumption might be linked to the spot price, but there is no possibility to own electricity spot as an asset (Vehvilainen, 2002). Thus, short-term supply and demand equilibrium determines the spot prices, which leads to that the current spot price does not automatically have anything to do with some future spot price (Weron, 2008).

Furthermore, the demand for electricity shows strong seasonality, mean-reverting behavior, high volatility and a right-skewness in the electricity spot price. The latter generates higher futures prices than the expected spot prices in the coming six months, i.e. contango (Bierbrauer et al., 2007). Weron (2008) claims that spot electricity prices are the best example of all

financial time series of anti-persistent data, i.e. mean reverting. Only on a daily level there is persistence in electricity spot price.

The unregulated electricity market opened in Norway in 1991 and became Nord Pool in 1993, Sweden joined in 1996, Finland in 1998 and Denmark became a part of it in 1999 (Weron et al., 2004). Despite that the Nordic countries have a well connected power grid there are still local differences in price due to transportation constraints of electricity. This in turn is the reason that Nord Pool is divided into a number of pricing areas, e.g. Sweden has four pricing areas where the prices in the north typically are lower than in the south due to greater supply combined with lower demand. There is a theoretical electricity spot price for the entire Nordic area called the system price. To smooth the differences in supply and demand for the different areas there are ongoing projects to connect the German, Baltic, Polish and even the British market further. The composition of electricity production also influences the spot price, i.e. how much hydro, nuclear, coal, wind power there is, respectively. For example, the increased amount of wind power has caused the spot price to sometimes become negative since it is sanctioned by the government and might thus be profitable to produce electricity even with negative a spot price (NordPool, 2015).

1.1.1 Seasonality

The seasonality effect on the electricity spot price is mainly due to the cyclical demand pattern, where the the demand is bigger for electricity during the winter because of lower temperature and less hours of daylight (Bierbrauer et al., 2007). Also the supply side might be influenced by the climate, mainly hydro power that is dependent on precipitation and snow melting, which have seasonal variations (Weron et al., 2004). Weron (2008) suggests that spot prices at Nord Pool have a sinusoid annual cycle and a linear trend, this is not as evident in other electricity markets, e.g. the German.

1.1.2 High volatility

The electricity spot price has a higher volatility than any other commodity, or other financial asset; there can be annualized volatilities of 1000% on hourly spot prices. In addition, it is not uncommon that electricity spot prices can have a daily standard deviation of 40%, compared to the stock market that has 1-2% (Bierbrauer et al., 2007).

1.1.3 Jumps and spikes

Price jumps occur because of sudden failure in the power grid that largely increases the prices in a very short amount of time. Spikes on the other hand occur due to a sudden increase in demand or when demand reaches the limit of the current capacity in the power grid. The spikes and jumps

can be explained by the highly non-linear supply-demand curve and the non-storability of electricity (Bierbrauer et al., 2007). After a jump, the electricity spot price generally reverts rapidly to a normal level and the high price does not last more than a day (Weron et al., 2004).

1.2 Dynamics of electricity derivatives

1.2.1 Forwards and futures

Electricity derivative contracts always imply delivery over a specified time period, unlike derivatives with stocks as the underlying asset, which are sold at a single point in time (Heppenger, 2012). Electricity forwards and futures are more like interest rate swaps than traditional forwards and futures. The underlying asset is the average spot price during a specified time period (Vehvilainen, 2002). The non-storability of electricity makes electricity futures contracts, with non-overlapping delivery intervals, seem to have different underlying assets/commodities. Unlike for most commodities there is no possibility to transfer one asset into the other, making hedging by commodity storage impossible (Hinz et al., 2005). Similarly as for the relationship between the current and a future spot price, no explicit connections exist for futures with different maturities (Weron, 2008).

Electricity futures display the Samuelson hypothesis¹, the volatility increases as the time to maturity decreases. When the delivery date approaches, the amount of information that affects the balance between supply and demand increases and thus makes the futures price more volatile (Goutte et al., 2014).

There are two main approaches to model electricity derivatives. The first one is to model the futures curve and from that deduce the spot price as futures with immediate delivery. However, this approach does not capture the right dependencies between fuels and electricity prices. The second approach computes the futures price as the expectation of the spot price under a risk neutral probability, i.e. starts with the spot price. This approach generates a consistent framework for all possible derivatives, but it leads to complex computations (Äid et al., 2013). Note that there is no replicating portfolio for physical spot electricity (Vehvilainen, 2002).

While the electricity spot market in the Nordic countries is provided by Nord Pool, the derivatives on electricity are provided by Nasdaq OMX. There are yearly, quarterly, monthly, weekly and daily futures contracts. Each contract size is 1MWh, but depending on the maturity, the contracts have different number of delivery hours. For example, the yearly futures contract has 8760 delivery hours (8784 hours in case of a leap year) (NASDAQOMX, 2015).

¹see Samuelson (1965).

Derivatives can be written on either peak load or base load prices. For base load, there are prices for 24 hours 7 days a week, while for peak load there are prices from 8 a.m. to 8 p.m. Monday to Friday. There are also off-peak prices, which simply are the prices for the non-peak hours. At Nasdaq OMX, both futures contracts on base load and on peak load are provided. However, the base load contracts are more liquid for the Nordic market, contrary to the German market where the peak load contracts are the most traded. The differences can be explained by the larger portion of hydro power in the Nordic market, which decreases the differences during peak and non-peak hours (NordPool, 2015). A large issue when trading with electricity derivatives is the liquidity. In the futures contracts 90% of the liquidity is in a few contracts. The most liquid contracts typically are the front month, the front quarter and the front year contracts. The front month contract refers to the futures contract with delivery period during the coming month, e.g. the front month contract in April is the May contract, and similarly for the front quarter and front year contract, respectively. The illiquidity leads to large spreads between the bid and ask price and to increased costs when trading these contracts (Forsell, 2015).

1.2.2 Options

There are two common options on electricity; European options written on the futures price and Asian options written on the spot price. The former is provided by Nasdaq OMX, the latter was previously provided by Nasdaq OMX, but has now been removed. Asian options written on electricity are settled against the arithmetic average hourly spot price during the delivery period, typically one month. The delivery period starts when the option expires, this makes Asian options on electricity differ from other financial Asian options, which are settled against the average price during the trading period of the option. The delivery period corresponds to the "underlying" futures contract. Settlement takes place the day after the delivery period has ended (Weron, 2008).

Asian options were more frequently traded before 2006 when the Nordic market changed and became more volatile. Now, Asian options, mostly calls, are issued by producers to hedge their own production. The seasonality of the spot electricity prices has effects on the risk when issuing Asian options as well, e.g. it is more risky to issue an Asian call option in the winter than in the summer. This is because of the large spikes that are more common during the winter (Forsell, 2015).

Weron (2008) presents a jump-diffusion model for modeling electricity spot price at Nord Pool. The model captures typical characteristics of the spot price such as seasonality, jumps and mean reversion. Further, he derives a pricing formula for Asian options written on the electricity spot price by calibrating the market price of risk.

1.2.3 Hedging Asian electricity options

Trading of the future is only possible up to the delivery period. When the delivery period has started, the positions in the hedge are fixed and cannot be adjusted anymore until maturity (Benth and Detering, 2014). Recall that there is no relationship between neither futures contracts with different maturities, nor spot prices at different times (Weron, 2008). This makes it hard to use other futures contracts to hedge the position during the delivery period of the option, when the corresponding futures contract is not possible to trade. For example, if the Asian option has a one month delivery period, the future with corresponding delivery month might be used for hedging. During the delivery period that future is not tradable, but there are weekly and daily futures for that period available. However, because there is no clear relationship between the contracts, it is theoretically difficult to use them as hedging instruments.

Several authors have written about the struggles of hedging electricity derivatives in general. The challenge is to hedge an option that depends on the infinite-dimensional futures curve, with a small number of contracts. For example, hedging an option with one year delivery period with weekly futures contracts. Taking this into account, Hepperger (2012) presents quadratic hedging strategies for European options on electricity swaps by modeling the futures curve with an exponential jump-diffusion process. Further, Vehvilainen (2002) states that it is impossible to perfectly hedge an Asian option using only the spot price and a bank account, or using electricity futures. This is because the electricity futures contract is only tradable up to the delivery period of the corresponding Asian option, but the payoff of the option depends on the events during delivery period. Dynamic adjustments of the hedging portfolio are not possible either (Vehvilainen, 2002). However, Benth and Detering (2014) present three different models for hedging Asian options on electricity with the trading restriction of the futures contracts taken into consideration.

1.3 Lévy processes

To model electricity prices Goutte et al. (2014), Benth and Detering (2014) and Barndorff-Nielsen and Shephard (2001), among others, suggest the use of Lévy processes. Their basic properties are presented here.

Suppose that we have a process Y_t where the distribution of Y_1 is \mathcal{D} . If we divide the time into n equal time intervals and assume that the increments are independent and from a common distribution $\mathcal{D}^{(n)}$, we can write Y_t as

$$Y_t^{(n)} = \sum_{j=1}^{\lfloor tn \rfloor} C_j^{(n)}$$

where $C_j^{(n)} \stackrel{i.i.d}{\sim} \mathcal{D}^{(n)}$. The sum will have distribution \mathcal{D} when $t = 1$. The distribution $\mathcal{D}^{(n)}$ depends on n , but the distribution of the sum (construction \mathcal{D}) does not. This is possible for processes where \mathcal{D} is infinitely divisible and the resulting process is called a Lévy process (Barndorff-Nielsen and Shephard, 2012).

The definition of a Lévy process is that a càdlàg stochastic process Y_t with zero initial value is a Lévy process if and only if it has independent and strictly stationary increments. This means that the distribution of $Y_{t+s} - Y_t$ may depend on s but not on t (the stationarity assumption). It also implies that the shocks to the process are independent over time. The stationarity and independent increments imply that the cumulant function of Y_t is only governed by the distribution of Y_1 :

$$\begin{aligned}\kappa_{Y_t}(\theta) &= \log E[e^{\theta Y_t}] \\ &= t \log E[e^{\theta Y_1}] \\ &= t \kappa_{Y_1}(\theta).\end{aligned}$$

A process is said to be càdlàg if the process is right continuous, with probability one,

$$\lim_{s \downarrow t} Y_s = Y_t$$

and has limits from the left

$$Y_{t-} = \lim_{s \uparrow t} Y_s.$$

The jump at time t can then be written as

$$\Delta Y_t = Y_t - Y_{t-}.$$

This means that a Lévy process allows jumps, contrary to stochastic processes that have continuous sample paths with probability one. These characteristics make a Lévy process a flexible framework when modeling asset returns. However, the returns will be independent and identically distributed when measured over a fixed time length, i.e. it ignores serial dependencies such as volatility clustering (Barndorff-Nielsen and Shephard, 2012).

Examples of Lévy processes are the Poisson, Gamma, Inverse Gaussian (IG), Wiener process, Normal Inverse Gaussian (NIG) and skewed Student's t process. The first three processes are non-negative Lévy processes, subordinators, which have non-negative increments. In this thesis the *NIG* distribution is used, some characteristics of it are presented below.

1.3.1 The *NIG* distribution

The normal inverse Gaussian distribution with tail-heaviness α , skewness β , location μ and scale δ is denoted $NIG(\alpha, \beta, \mu, \delta)$. The *NIG* distribution can model both asymmetric and symmetric distributions as well as long tails in both directions. Because of this, it is suitable for modeling various types of log returns in finance. The tails of the *NIG* distribution is considered semi-heavy. They are definitely heavier than the tails of a Gaussian distribution, but not as heavy as for a Pareto distribution. The density function of the *NIG* distribution is

$$f(x; \alpha, \beta, \mu, \delta) = a(\alpha, \beta, \mu, \delta) q\left(\frac{x - \mu}{\delta}\right)^{-1} K_1\left(\delta \alpha q\left(\frac{x - \mu}{\delta}\right)\right) e^{\beta x}$$

with $q(x) = \sqrt{1 + x^2}$, $a(\alpha, \beta, \mu, \delta) = \pi^{-1} \alpha e^{\delta \sqrt{\alpha^2 - \beta^2} - \beta \mu}$ and with K_1 is the modified Bessel function of the third order and index 1 (Barndorff-Nielsen, 1997).

1.4 Problem formulation

There is a demand for Asian electricity options from the industry. The characteristics of the electricity spot price, the non-storability of electricity in particular, make it difficult for the issuer to hedge the market risk when issuing Asian options. To cover for the uncertainty of the hedge the issuer needs to add a fee, which increases the price of the option and thus decreases the demand for the option. It is therefore of interest to evaluate hedging strategies for Asian options. A better model for the hedging strategy would reduce the risk for the issuer and decrease the price of the option for the buyer.

This is an empirical analysis based on the system spot prices from Nord Pool between 2006 and 2014 as well as futures contract prices between 2010 and 2014. The evaluation of hedging strategies is made by comparing the tracking and hedging error for a simple quadratic hedging strategy (in many ways similar to a delta hedge) with a more complex quadratic hedging strategy. The aim is to minimize the tracking error. To get a more nuanced picture of the distribution of the tracking error, value at risk of the tracking error is presented. In addition, a third model is presented that accounts for several of the spot price's characteristics. This model is evaluated in Benth and Detering (2014) but not included in the empirical evaluation in this thesis. The thesis focuses on evaluation of hedging strategies for Asian call options.

Hedging strategies:

1. Quadratic hedge using the Black-Scholes framework with the future price process modeled as a geometric Brownian motion.
2. Quadratic hedge with the future price process modeled with stochastic volatility.
3. Quadratic hedge with the future price process modeled as an exponential additive process.

Evaluation criteria:

- Minimize the tracking error.
- Investigate tracking error by empirical VaR, minimum and maximum of tracking error.

The thesis is based on Benth and Detering (2014)'s paper, but with more focus on comparing the first two models through empirically investigating the tracking error. This thesis uses base load prices instead of peak load prices as Benth and Detering (2014) used. The parameters are estimated through historical data and the evaluation of the models is based on out-of-sample data, i.e. the evaluation of models is not based on the same historical data as the parameters are estimated on.

The Chapter 2 presents three different ways to model electricity futures prices and corresponding hedging strategies for Asian options on electricity spot price. It starts with a rather simple geometric Brownian motion and the Black-Scholes framework, but includes the trading restrictions of the futures contract. A process with stochastic volatility follows, where the hedging positions are derived from Laplace transforms. The third model is an exponential additive process which accounts for seasonality and jumps in the spot price. In Chapter 3 data analysis of the historical spot and futures prices are provided along with methods for estimating the parameters for the two first models. In Chapter 4 there is the result of the tracking and hedging error from hedging an Asian option, when the futures price is simulated by a geometric Brownian motion and a stochastic volatility model, respectively. Finally, Chapter 5 contains conclusions drawn from the results in Chapter 3 and Chapter 4.

Chapter 2

Theory

Here three models for hedging Asian options written on the electricity spot price are presented. Firstly, the future price process is modeled as a geometric Brownian motion with time dependent volatility. Secondly, the future price process is modeled by a stochastic volatility process. Finally, an exponential additive process is presented for modeling the spot price process as well as the futures price process. Explicit expressions for the price of the Asian option and corresponding hedging positions are presented for each model.

2.1 Assumptions and definitions

Let us start with defining the underlying process, the payoff function of an Asian option and the hedging portfolio. Throughout this thesis, interest rates are assumed to be zero. It is also assumed that the underlying contract is impossible to trade during the delivery period, i.e. after time T_1 .

The futures contracts are defined as the arithmetic average of the spot price over a specified time period called the delivery period. The future price process is defined as follows.

Definition 2.1 *Future price process*

Let the adaptive process $(X_t)_{0 \leq t \leq T_2}$ represent the future price process of a futures contract with the payout at time T_2

$$X_{T_2} = \frac{1}{T_2 - T_1} \int_{T_1}^{T_2} S_r \, dr$$

where $(S_t)_{0 \leq t \leq T_2}$ is the spot electricity price. The futures contract has delivery period $[T_1, T_2]$ and is only possible to trade up to time T_1 .

The aim of this thesis is to evaluate hedging strategies for Asian options, in order to do that we need to be able to price the options. However, pricing

formulas for Asian options are in general complex. Given the futures price process in Definition 2.1 we can rewrite an Asian option written on the spot price as a European option written on the futures price, which gives more straight-forward pricing formulas.

Definition 2.2 Asian option

Let $C(X_{T_2}) := (X_{T_2} - K)^+$ be the payoff of a European call option written on the future price process X_t . The payoff of an Asian call option written on the electricity spot price is

$$\left(\frac{1}{T_2 - T_1} \int_{T_1}^{T_2} S_r \, dr - K \right)^+.$$

Note that $C(X_{T_2})$ has the same payoff as the Asian call option, $C(X_{T_2})$ can thus be regarded as an Asian call option on the spot price. Similarly, let $P(X_{T_2})$ be the payoff of a European put option written on the futures price, which will have the same payoff as an Asian put option on the spot. Further, let $C(t, T_1, T_2)$ and $P(t, T_1, T_2)$ denote the price of the call option and put option, respectively, at time t . If we assume no arbitrage, two different claims with the same payoff must have the same price¹. In this way, we can focus on pricing the simpler European option on the futures contract, instead of the Asian option on the spot price.

The hedging constraint of the futures contract, that it is only possible to trade up to the delivery period, affects the hedging strategy. The constraint leads to that the last position entered in the hedging portfolio must take the expectation of the entire delivery period into consideration. The hedging portfolio consists therefore of the initial capital, the continuous hedging positions that can be taken before the delivery period (i.e. before time T_1), and the hedging position taken at time T_1 that should cover the entire delivery period. This type of hedging constraint is considered in Benth and Detering (2014) and they derive a solution to the quadratic hedging problem.

Definition 2.3 Hedging portfolio

We assume that trading is continuously possible when $t \in [0, T_1]$ but that the hedging positions are constant when $t \in [T_1, T_2]$. Let the hedging portfolio V_t at time t be

$$V_t = V_0 + \int_0^{T_1 \wedge t} \psi_s \, dX_s + \mathbb{1}_{t > T_1} \psi_{T_1} (X_t - X_{T_1})$$

where ψ_t denotes the continuous hedge position up to time T_1 and ψ_{T_1} is the hedge position taken just before the delivery period of the underlying asset (in this case a futures contract). We want to find a portfolio V_t that minimizes

¹Otherwise it would always be possible to buy the cheaper claim and sell the more expensive, gaining the difference in the present with no risk for loss in the future.

$$E\left[(H - V_{T_2})^2\right]$$

where H is the claim at time T_2 , e.g. $C(X_{T_2})$.

Benth and Detering (2014) show that the continuous hedging positions up to time T_1 are the same as for the hedging portfolio with no constraint. Further, they derive the hedging position at time T_1 , which is specified below.

Proposition 2.4 *Let H be an \mathcal{F}_{T_2} -measurable payoff with $E[H^2] < \infty$ and V_{T_1} the value of the portfolio at time T_1 . Also, let M be a martingale. Then the hedging position ψ_{T_1} that minimizes $E[(H - V_{T_1} - \zeta(M_{T_2} - M_{T_1}))]$ with respect to ζ , is given by*

$$\psi_{T_1} = \frac{E[(H)(M_{T_2} - M_{T_1})|\mathcal{F}_{T_1-}]}{E[(M_{T_2} - M_{T_1})^2|\mathcal{F}_{T_1-}]}.$$

Note that ψ_{T_1} does not depend on the portfolio value at time T_1 .

Further, the optimal hedging position ψ_t at time $t < T_1$ is given by the optimal hedging position without the hedging restrictions. V_0 is the initial capital and is equal to the price of the claim at time 0

$$V_0 = E[H].$$

Proof. See Proposition 2.4 and 2.7 in Benth and Detering (2014). □

The general expressions for the future price process and the hedging portfolio, respectively, are specified in the following three models. Also, explicit formulas for pricing Asian options on electricity spot price are presented.

2.2 Geometric Brownian motion

First of the three models presented in this thesis is a geometric Brownian motion with time dependent volatility. Here it is possible to use the classic Black-Scholes framework for option pricing and delta hedging. Also, proofs are presented for a better understanding of the model and the hedging strategy. The geometric Brownian motion model is simpler than the following two models, which makes it more transparent and requires less running time. The geometric Brownian motion with time dependent volatility is suggested for modeling electricity by Benth and Detering (2014) as well as Lucia and Schwartz (2002).

2.2.1 Modeling futures prices

The future price process $(X_t)_{0 \leq t \leq T_2}$ in Definition 2.1 is here a geometric Brownian motion and given by the SDE

$$dX_t = \sigma(t)X_t dW_t \quad (2.1)$$

where W_t is a Wiener process. The volatility is expressed as a deterministic function of time $\sigma(t) = \hat{\sigma} \exp\{-\alpha(T_2 - t)\}$, where $\hat{\sigma}$ and α are constants and T_2 is the maturity of the future. This was suggested by Lucia and Schwartz (2002) for electricity futures and is consistent with the Samuelson effect. The process X_t is given by

$$X_t = X_s \exp\left\{ \int_s^t \sigma(u) dW_u - \frac{1}{2} \int_s^t \sigma^2(u) du \right\}. \quad (2.2)$$

Let $\tilde{\sigma}_{s,t}^2 = \int_s^t \sigma^2(u) du$, then we have that the log return is normally distributed $\log(X_t/X_s) \sim N\left(-\frac{1}{2}\tilde{\sigma}_{s,t}^2, \tilde{\sigma}_{s,t}^2\right)$, where $\tilde{\sigma}_{s,t}^2$ is the variance (Jean-Pierre et al., 2000). Note that

$$\begin{aligned} \tilde{\sigma}_{s,t}^2 &= \int_s^t \hat{\sigma}^2 e^{-2\alpha(T_2-u)} du \\ &= \frac{\hat{\sigma}^2}{2\alpha} \left(e^{-2\alpha(T_2-t)} - e^{-2\alpha(T_2-s)} \right). \end{aligned} \quad (2.3)$$

2.2.2 Option pricing

Since X_t is a geometric Brownian motion we can use the classic Black-Scholes framework for option pricing.

Proposition 2.5 *The price of a call and a put option will just be given by the Black-Scholes formula for European options, with volatility parameter $\sqrt{\tilde{\sigma}_{t,T_2}^2/(T_2 - t)}$,*

$$\begin{aligned} C(t, T_1, T_2) &= E\left[(X_{T_2} - K)^+ | \mathcal{F}_t\right] = X_t \Phi(d_1) - K \Phi(d_2) \\ P(t, T_1, T_2) &= E\left[(K - X_{T_2})^+ | \mathcal{F}_t\right] = K \Phi(-d_2) - X_t \Phi(-d_1) \end{aligned}$$

with

$$\begin{aligned} d_1 &= \frac{\log(X_t/K) + \frac{1}{2}\tilde{\sigma}_{t,T_2}^2}{\tilde{\sigma}_{t,T_2}} \\ d_2 &= d_1 - \tilde{\sigma}_{t,T_2} \end{aligned}$$

where $\Phi(x)$ denotes the cumulative standard normal distribution function, K denotes the strike price and $\tilde{\sigma}_{t,T_2}^2$ is defined as in Equation (2.3).

Remark 2.6 Recall that a European option on the future price process X_t will have the same payoff as an Asian option on the spot price S_t . Due to the no arbitrage assumption, two different options with the same payoff must have same price. See Definition 2.2.

2.2.3 Hedging positions

We want to get explicit formulas for the three hedging positions in Definition 2.3. The three positions are the initial capital, the continuous hedging position and the position at time T_1 . The initial capital is simply the price of the option at time 0, where the option price is given by Proposition 2.5. The positions for the hedging portfolio V_t up to time T_1 , i.e. the continuous hedging positions, are given by the usual Black-Scholes delta,

$$\begin{aligned}\psi_t^{call} &= \Phi(d_1) \\ \psi_t^{put} &= 1 - \Phi(d_1)\end{aligned}$$

where d_1 is defined as in Proposition 2.5. The hedging position at time T_1 is given by the following Proposition, the formula is derived by Benth and Detering (2014).

Proposition 2.7 The hedging position at time $t = T_1$ for a call option with payoff $C(X_{T_2})$ is given by

$$\psi_{T_1}^{call} = \frac{X_{T_1} e^{\tilde{\sigma}_{T_1, T_2}^2} (2\tilde{\sigma}_{T_1, T_2} - \tilde{K}) - (K + X_{T_1})\Phi(\tilde{\sigma}_{T_1, T_2} - \tilde{K}) + K\Phi(-\tilde{K})}{X_{T_1} (e^{\tilde{\sigma}_{T_1, T_2}^2} - 1)}$$

where

$$\tilde{K} = \frac{\log(K/X_{T_1}) + \frac{1}{2}\tilde{\sigma}_{T_1, T_2}^2}{\tilde{\sigma}_{T_1, T_2}}$$

and $\tilde{\sigma}_{T_1, T_2}^2$ is defined as in Equation (2.3). The corresponding hedge position for a put option is $\psi_{T_1}^{put} = \psi_{T_1}^{call} - 1$.

Proof. We know from Proposition 2.4 that the hedge position at time T_1 is given by $E[C(X_{T_2})(X_{T_2} - X_{T_1})|\mathcal{F}_{T_1-}]/E[(X_{T_2} - X_{T_1})^2|\mathcal{F}_{T_1-}]$. Note that since we have a continuous future price process X_t the filtration \mathcal{F}_{T_1} will be the same as the filtration \mathcal{F}_{T_1-} . Let us start with computing the numerator.

$$\begin{aligned}
& E[C(X_{T_2})(X_{T_2} - X_{T_1})|\mathcal{F}_{T_1}] \\
&= \int_{-\infty}^{\infty} C(X_{T_1}e^{-\frac{\tilde{\sigma}_{T_1, T_2}^2}{2} + \tilde{\sigma}_{T_1, T_2}y})(X_{T_1}e^{-\frac{\tilde{\sigma}_{T_1, T_2}^2}{2} + \tilde{\sigma}_{T_1, T_2}y} - X_{T_1})\frac{1}{\sqrt{2\pi}}e^{-\frac{y^2}{2}} dy \\
&= \int_{\tilde{K}}^{\infty} C(X_{T_1}e^{-\frac{\tilde{\sigma}_{T_1, T_2}^2}{2} + \tilde{\sigma}_{T_1, T_2}y})(X_{T_1}e^{-\frac{\tilde{\sigma}_{T_1, T_2}^2}{2} + \tilde{\sigma}_{T_1, T_2}y} - X_{T_1})\frac{1}{\sqrt{2\pi}}e^{-\frac{y^2}{2}} dy
\end{aligned} \tag{2.4}$$

since the integrand is zero for $y < \tilde{K}$. Let us begin with computing the first summand of the integral to avoid too long expressions.

$$\begin{aligned}
& \int_{\tilde{K}}^{\infty} (X_{T_1}e^{-\frac{\tilde{\sigma}_{T_1, T_2}^2}{2} + \tilde{\sigma}_{T_1, T_2}y} - K)X_{T_1}e^{-\frac{\tilde{\sigma}_{T_1, T_2}^2}{2} + \tilde{\sigma}_{T_1, T_2}y}\frac{1}{\sqrt{2\pi}}e^{-\frac{y^2}{2}} dy \\
&= X_{T_1}^2 e^{\tilde{\sigma}_{T_1, T_2}^2} \int_{\tilde{K}}^{\infty} e^{-\frac{1}{2}(y-2\tilde{\sigma}_{T_1, T_2})^2} \frac{1}{\sqrt{2\pi}} dy - KX_{T_1} \int_{\tilde{K}}^{\infty} e^{-\frac{1}{2}(y-\tilde{\sigma}_{T_1, T_2})^2} \frac{1}{\sqrt{2\pi}} dy \\
&= X_{T_1}^2 e^{\tilde{\sigma}_{T_1, T_2}^2} \int_{\tilde{K}-2\tilde{\sigma}_{T_1, T_2}}^{\infty} e^{-\frac{1}{2}x^2} \frac{1}{\sqrt{2\pi}} dx - KX_{T_1} \int_{\tilde{K}-\tilde{\sigma}_{T_1, T_2}}^{\infty} e^{-\frac{1}{2}x^2} \frac{1}{\sqrt{2\pi}} dx
\end{aligned} \tag{2.5}$$

recall that $\Phi(x) = 1 - \Phi(-x)$, Equation (2.5) can then be written as

$$X_{T_1}^2 e^{\tilde{\sigma}_{T_1, T_2}^2} \Phi(2\tilde{\sigma}_{T_1, T_2} - \tilde{K}) - KX_{T_1} \Phi(\tilde{\sigma}_{T_1, T_2} - \tilde{K}).$$

Similarly, the second summand in (2.4) becomes

$$-X_{T_1}^2 \Phi(\tilde{\sigma}_{T_1, T_2} - \tilde{K}) + KX_{T_1} \Phi(-\tilde{K}).$$

Finally,

$$E[(X_{T_2} - X_{T_1})^2|\mathcal{F}_{T_1}] = X_{T_1}^2 (e^{\tilde{\sigma}_{T_1, T_2}^2} - 1)$$

gives Proposition 2.7. \square

2.3 Stochastic volatility

In the second model, the future price process is just like the geometric Brownian motion driven by a Wiener process, but it has stochastic volatility. The model has been proposed in Benth and Detering (2014) and for gas prices in Benth (2011). Originally, Barndorff-Nielsen and Shephard (2001) presented this model, but with an application for the currency market. Explicit formulas for option pricing and hedging positions are presented using inverse Laplace transforms. Here some proofs are presented for better understanding of the model, but details of the derivation of the Laplace transforms are left out.

2.3.1 Modeling spot and futures prices

The futures price process $(X_t)_{0 \leq t \leq T_2}$ in Definition 2.1 is here given by the SDE

$$dX_t = X_t \sigma_t dB_t \quad (2.6)$$

where B_t is a Wiener process and with the stochastic volatility σ_t . Let $Y_t = \sigma_t^2$ be given by

$$dY_t = -\lambda_t Y_t dt + dL_t \quad (2.7)$$

where λ_t is assumed to be deterministic and positive, and L_t is a finite subordinator process² without deterministic drift. That is, Y_t will be positive and σ_t will be well defined for all Y_t . Since L_t is a pure jump Lévy process it will be independent of B_t , and therefore also the stochastic volatility σ_t will be independent of B_t . The process Y_t is an Ornstein-Uhlenbeck process and Equation (2.7) has thus the solution

$$Y_u = Y_t e^{-\int_t^u \lambda_r dr} + \int_t^u e^{-\int_s^u \lambda_r dr} dL_s. \quad (2.8)$$

The solution to Equation (2.6) is

$$X_t = X_s \exp \left\{ -\frac{1}{2} \int_s^t \sigma_u^2 du + \int_s^t \sigma_u dB_u \right\}. \quad (2.9)$$

We would like to have an easier expression for the integrated variance in Equation (2.9). If we integrate Equation (2.8) over $[t, T]$ we get

$$\int_t^T \sigma_u^2 du = Y_t \int_t^T e^{-\int_t^u \lambda_r dr} du + \int_t^T \int_t^u e^{-\int_s^u \lambda_r dr} dL_s du.$$

To obtain the integrated variance we use the Fubini theorem, as in Benth and Detering (2014), and get

$$\int_t^T \sigma_u^2 du = \sigma_t^2 \epsilon(t, T) + \int_t^T \epsilon(u, T) dL_u, \quad (2.10)$$

with continuous function

$$\epsilon(t, T) = \int_t^T e^{-\int_t^u \lambda_r dr} du. \quad (2.11)$$

Note that if $\lambda_t = \lambda$ is a constant for all t we get $\epsilon(t, T) = \lambda^{-1}(1 - e^{-\lambda(T-t)})$. The constant λ will be used for empirically evaluate the stochastic volatility

²An increasing Lévy process with non negative increments (see Barndorff-Nielsen and Shephard (2012)).

model in Chapter 3 and Chapter 4. Further, let Z_t denote the log price process of X_t

$$Z_t := \log X_t = \log X_0 - \frac{1}{2} \int_0^t \sigma_s^2 ds + \int_0^t \sigma_s dB_s. \quad (2.12)$$

This allows us to derive the Laplace transform of the distribution of Z_t , and using that we can price derivatives on X_t . First, we need the cumulant function of the Lévy process L_t . Let the Lévy measure $w(x)$ of L_t be such that the cumulant function $\kappa(\theta) = \log E[e^{\theta L_1}]$ exists for $\theta \in (-b, b)$

$$\kappa(\theta) = \int_0^\infty (e^{\theta x} - 1)w(x) dx. \quad (2.13)$$

The lemma below is proved in Nicolato and Venardos (2003) for a constant λ and derived for a deterministic time dependent function λ_t by Benth and Detering (2014).

Lemma 2.8 *The Laplace transform $\phi(t, T, z, \sigma_t) = E[\exp\{z(Z_T - Z_t)\} | \sigma_t]$ is given by*

$$\phi(t, T, z, \sigma_t) = \exp\left\{\frac{1}{2}(z^2 - z)\sigma_t^2 \epsilon(t, T) + \int_t^T \kappa(f(s, z)) ds\right\}$$

with $f(s, z) := \frac{1}{2}(z^2 - z)\epsilon(s, T)$, $\kappa(\theta)$ and $\epsilon(t, T)$ defined as in Equation (2.13) and (2.11), respectively. The transform is well defined in the stripe $\mathcal{S} = \{\Re(z) \in (\theta_-, \theta_+)\}$ with

$$\begin{aligned} \theta_+ &= \frac{1}{2} + \sqrt{\frac{1}{4} + 2b\epsilon(t, T)^{-1}}, \\ \theta_- &= -\frac{1}{2} - \sqrt{\frac{1}{4} + 2b\epsilon(t, T)^{-1}}. \end{aligned}$$

To be able to price calls and puts we need the (bilateral) Laplace transform for the payoff functions of call and put options. The Laplace transform is defined by

$$\mathcal{L}\{f(y)\}(z) = \int_{-\infty}^{\infty} f(t)e^{-zt} dt.$$

The subsequent lemma is proved in Benth and Detering (2014) and gives the Laplace transforms for the payoff and modified payoff functions for call and put options, respectively. The payoff functions are needed for the option prices and the continuous hedging positions. The modified payoff functions are needed for the hedging position at time T_1 .

Lemma 2.9 *Let*

$$L_1(z) = X_t^z \frac{K^{1-z}}{z(z-1)}$$

$$L_2(z) = -\frac{X_{T_1}^2}{2-z} \left(\frac{K}{X_{T_1}}\right)^{2-z} + \frac{KX_{T_1} + X_{T_1}^2}{1-z} \left(\frac{K}{X_{T_1}}\right)^{1-z} + \frac{KX_{T_1}}{z} \left(\frac{K}{X_{T_1}}\right)^{-z}$$

and

$$c_1(y) = (X_t e^y - K)^+$$

$$p_1(y) = (K - X_t e^y)^+$$

$$c_2(y) = (X_{T_1} e^y - K)^+ (X_{T_1} e^y - X_{T_1})$$

$$p_2(y) = (K - X_{T_1} e^y)^+ (X_{T_1} e^y - X_{T_1})$$

Then

$$L_1(z) = \begin{cases} \mathcal{L}\{c_1(y)\}(z) & \text{for } z \text{ with } \Re(z) > 1 \\ \mathcal{L}\{p_1(y)\}(z) & \text{for } z \text{ with } \Re(z) < 0 \end{cases}$$

$$L_2(z) = \begin{cases} \mathcal{L}\{c_2(y)\}(z) & \text{for } z \text{ with } \Re(z) > 2 \\ \mathcal{L}\{p_2(y)\}(z) & \text{for } z \text{ with } \Re(z) < -2. \end{cases}$$

Benth and Detering (2014) suggest to model daily log returns of electricity futures with a *NIG* distribution. The *NIG* distribution is also used by Benth (2011) for the squared stochastic volatility of gas spot prices in the UK. This indicates that the *NIG* distribution might be useful when modeling the squared stochastic volatility for the electricity future price process X_t . Barndorff-Nielsen and Shephard (2001) show that if the subordinator process L_t , which drives Y_t , has *IG* distributed marginals, Y_t will be *NIG* distributed. In this case we can derive explicit formulas for Equation (2.13) and $\phi(t, T, z, \sigma_t)$ in Lemma 2.8. If we let $L_t \sim IG(\delta, \gamma)$, $\kappa(\theta)$ in Equation (2.13) becomes

$$\kappa(\theta) = \delta\gamma - \delta(\gamma^2 - 2\theta)^{1/2}. \quad (2.14)$$

Further, Nicolato and Venardos (2003) presents a closed form solution for the integral in Lemma 2.8 for a constant $\lambda_t = \lambda$

$$\int_t^T \kappa(f(s, z)) ds = \frac{\delta}{\lambda} \left(\sqrt{\gamma^2 - 2f_1} - \gamma \right) + \frac{2\delta f_2}{\lambda \sqrt{2f_2 - \gamma^2}}$$

$$\times \left(\arctan \left(\frac{\gamma}{\sqrt{2f_2 - \gamma^2}} \right) - \arctan \left(\sqrt{\frac{\gamma^2 - 2f_1}{2f_2 - \gamma^2}} \right) \right)$$

with $f_1 = \frac{1}{2}(z^2 - z)(1 - e^{-\lambda(T-t)})$ and $f_2 = \frac{1}{2}(z^2 - z)$. We can then write $\phi(t, T, z, \sigma_t)$ as

$$\begin{aligned} \phi(t, T, z, \sigma_t) = & \exp \left\{ \frac{1}{2}(z^2 - z)\sigma_t^2 \lambda^{-1}(1 - e^{-\lambda(T-t)}) \right. \\ & + \frac{\delta}{\lambda} \left(\sqrt{\gamma^2 - 2f_1} - \gamma \right) + \frac{2\delta f_2}{\lambda \sqrt{2f_2 - \gamma^2}} \\ & \left. \times \left(\arctan \left(\frac{\gamma}{\sqrt{2f_2 - \gamma^2}} \right) - \arctan \left(\sqrt{\frac{\gamma^2 - 2f_1}{2f_2 - \gamma^2}} \right) \right) \right\}. \end{aligned}$$

This is used in Chapter 3 and 4 when empirically evaluating the hedging strategy based on the stochastic volatility model.

2.3.2 Option pricing

To derive an integral representation of the price for put and call options under the process (2.6), we use the Laplace transform of the options's payoffs $L_1(z)$ in Lemma 2.9 and the Laplace transform of the incremental log price density in Lemma 2.8.

Proposition 2.10 *The price of a call and a put option, respectively, at time t is*

$$\begin{aligned} C(t, T_1, T_2) &= \frac{1}{2\pi i} \int_{c-i\infty}^{c+i\infty} X_t^z \frac{K^{1-z}}{z(z-1)} \phi(t, T_2, z, \sigma_t) dz, \quad c > 1 \\ P(t, T_1, T_2) &= \frac{1}{2\pi i} \int_{c-i\infty}^{c+i\infty} X_t^z \frac{K^{1-z}}{z(z-1)} \phi(t, T_2, z, \sigma_t) dz, \quad c < 0 \end{aligned}$$

with $\phi(t, T_2, z, \sigma_t)$ defined as in Lemma 2.8.

Proof. This proof is presented in Benth and Detering (2014) and shows how the inverse of a Laplace transformation can be used for pricing options. Let us consider the call option. We want to compute

$$E \left[(X_{T_2} - K)^+ | \mathcal{F}_t \right] = E \left[c_1(Z_{T_2} - Z_t) | \mathcal{F}_t \right] \quad (2.15)$$

with $c_1(y)$ as in Lemma 2.9. Since $c_1(y)$ is of bounded variation on compacts and $\mathcal{L}\{c_1(y)\}(z)$ is well defined for $\Re(z) = c$ we can use the Laplace inversion theorem

$$g(y) = \frac{1}{2\pi i} \int_{c-i\infty}^{c+i\infty} \mathcal{L}\{g(y)\}(z) e^{zy} dz.$$

Using this we can compute (2.15) by changing the order of integration and noting that the line of integration lies within the set \mathcal{S} defined in Lemma 2.8

$$\begin{aligned}
E\left[c_1(Z_{T_2} - Z_t) | \mathcal{F}_t\right] &= \frac{1}{2\pi i} E\left[\int_{c-i\infty}^{c+i\infty} \mathcal{L}\{c_1(y)\}(z) e^{z(Z_{T_2} - Z_t)} dz | \mathcal{F}_t\right] \\
&= \frac{1}{2\pi i} \int_{c-i\infty}^{c+i\infty} \mathcal{L}\{c_1(y)\}(z) E\left[e^{z(Z_{T_2} - Z_t)} | \mathcal{F}_t\right] dz \\
&= \frac{1}{2\pi i} \int_{c-i\infty}^{c+i\infty} \mathcal{L}\{c_1(y)\}(z) \phi(t, T_2, z, \sigma_t) dz
\end{aligned}$$

where $\phi(t, T_2, z, \sigma_t)$ is the Laplace transform of the incremental log price density derived in Lemma 2.8. \square

Remark 2.11 *Recall that a European option on the future price process X_t will have the same payoff as an Asian option on the spot price S_t . Due to the no arbitrage assumption, two different options with the same payoff must have same price. See Definition 2.2.*

2.3.3 Quadratic hedge

We want to determine the initial capital, the continuous hedging position and the hedging position at time T_1 for the hedging portfolio V_t in Definition 2.3. The initial capital V_0 is the initial value of the option and is computed according to Proposition 2.10. Benth and Detering (2014) show that the continuous hedging position is given by the derivative of the option with respect to the underlying price process. Just as when pricing the options in Proposition 2.10, the Laplace transforms of the payoff of the options as well as the incremental log price density are used when deriving a formula for the continuous hedging position.

Proposition 2.12 *The continuous hedge position for call and put payoffs for time (t, T_1) is given by*

$$\begin{aligned}
\psi_t^{call} &= \frac{\partial C(t, T_1, T_2)}{\partial X_t} = \frac{1}{2\pi i} \int_{c-i\infty}^{c+i\infty} \frac{1}{z-1} \left(\frac{K}{X_t}\right)^{1-z} \phi(t, T_2, z, \sigma_t) dz, \quad c > 1 \\
\psi_t^{put} &= \frac{\partial P(t, T_1, T_2)}{\partial X_t} = \frac{1}{2\pi i} \int_{c-i\infty}^{c+i\infty} \frac{1}{z-1} \left(\frac{K}{X_t}\right)^{1-z} \phi(t, T_2, z, \sigma_t) dz, \quad c < 0.
\end{aligned}$$

Proof. See Benth and Detering (2014) Proposition 3.6 and Corollary 3.7. \square

The hedging position at time T_1 is computed in a similar way as the option price and continuous hedging positions.

Proposition 2.13 *The hedging position for time $t = T_1$ is*

$$\psi_{T_1} = \frac{\frac{1}{2\pi i} \int_{c-i\infty}^{c+i\infty} \mathcal{L}\{g(y)\}(z) \phi(T_1, T_2, z, \sigma_t) dz}{E[(X_{T_2} - X_{T_1})^2 | \mathcal{F}_{T_1}]} \quad (2.16)$$

where $g(y) := f(X_{T_1} e^y)(X_{T_1} e^y - X_{T_1})$, and $f(X_{T_1} e^y)$ is a payoff function such that the Laplace transform of $g(y)$ is well defined in the stripe $\mathcal{R} := \{b_1 \leq \Re(z) \leq b_2\}$, $\mathcal{S} \cap \mathcal{R} \neq \emptyset$, with \mathcal{S} defined as in Lemma 2.8. The denominator of Equation (2.16) is

$$E[(X_{T_2} - X_{T_1})^2 | \mathcal{F}_{T_1}] = X_{T_1}^2 \left(e^{\sigma_{T_1}^2 \epsilon(T_1, T_2) + \int_{T_1}^{T_2} \kappa(\epsilon(s, T_2)) ds} - 1 \right) \quad (2.17)$$

where $\kappa(\theta)$ and $\epsilon(t, T)$ are defined as in Equation (2.13) and (2.11), respectively. For a call option $g(y) = c_2(y)$ and for a put option $g(y) = p_2(y)$, with their Laplace transforms defined in Lemma 2.9.

Proof. This proof is presented in Benth and Detering (2014). We know from Proposition 2.4 that $\psi_{T_1} = \frac{E[H(X_{T_2} - X_{T_1}) | \mathcal{F}_{T_1-}]}{E[(X_{T_2} - X_{T_1})^2 | \mathcal{F}_{T_1-}]}$. The proof for the numerator is similar to the proof for Proposition 2.10. To calculate the denominator, i.e. Equation (2.17), we need to introduce the filtration $\mathcal{G}_t := \sigma_t\{\sigma_s^2, 0 \leq s \leq T_2\} \vee \mathcal{F}_t$. Recall that σ_t^2 is independent of B_t . Due to the martingale property of X_t we obtain

$$E[(X_{T_2} - X_{T_1})^2 | \mathcal{F}_{T_1-}] = E[X_{T_2}^2 | \mathcal{F}_{T_1-}] - X_{T_1}^2.$$

We have $X_{T_2}^2 = X_{T_1}^2 e^{-\int_{T_1}^{T_2} \sigma_s^2 ds + \int_{T_1}^{T_2} 2\sigma_s dB_s}$ and thus

$$\begin{aligned} E[X_{T_2}^2 | \mathcal{F}_{T_1-}] &= X_{T_1}^2 E[e^{-\int_{T_1}^{T_2} \sigma_s^2 ds + \int_{T_1}^{T_2} 2\sigma_s dB_s} | \mathcal{F}_{T_1-}] \\ &= X_{T_1}^2 E[e^{-\int_{T_1}^{T_2} \sigma_s^2 ds} E[e^{\int_{T_1}^{T_2} 2\sigma_s dB_s} | \mathcal{G}_{T_1} | \mathcal{F}_{T_1-}]] \\ &= X_{T_1}^2 E[e^{\int_{T_1}^{T_2} \sigma_s^2 ds} | \mathcal{F}_{T_1-}] \\ &= X_{T_1}^2 e^{\sigma_{T_1}^2 \epsilon(T_1, T_2)} E[e^{\int_{T_1}^{T_2} \kappa(\epsilon(s, T_2)) dL_s} | \mathcal{F}_{T_1-}] \\ &= X_{T_1}^2 e^{\sigma_{T_1}^2 \epsilon(T_1, T_2) + \int_{T_1}^{T_2} \kappa(\epsilon(s, T_2)) dL_s} \end{aligned}$$

where Equation (2.10) gives the second last equality. The last equality follows from Lemma 3.1 in Eberlein and Raible (1999) and since $\epsilon(s, T)$ is continuous in s and bounded. $\kappa(\theta)$ and $\epsilon(t, T)$ are defined in Equation (2.13) and (2.11), respectively. \square

2.4 Exponential additive process

In the third model both the spot price and the future price process are modeled as exponential additive processes. The model starts with the spot price and from that deduces the future price process, unlike the two previous models that model the future price process immediately. A disadvantage with the first two models is that there is no data during the delivery period of the futures contracts, i.e. it is not possible to know how the future price process behave during the delivery period. When starting with the spot price, it is possible to get data for the entire period and thus bypassing the issue with lack of information during the delivery period for the future price process. This model was proposed and empirically tested by Benth and Detering (2014). It is not empirically tested in this thesis, but is included in the theory section as an example of a different approach of how to model the future price process.

2.4.1 Modeling spot and futures prices

Let us start with defining an additive stochastic process. An additive process is similar to a Lévy process, but the condition of stationarity of increments is relaxed. It is defined as

Definition 2.14 *A stochastic process Z_t is additive if it has the properties below*

1. $\mathbb{P}(Z_0 = 0) = 1$
2. *Independent increments, i.e. $Z_{t_i} - Z_{t_{i-1}}, Z_{t_j} - Z_{t_{j-1}}$ are independent for any $i \neq j$*
3. *Stochastic continuity, i.e. $\forall \epsilon > 0, \lim_{h \rightarrow 0} \mathbb{P}(|Z_{t+h} - Z_t| \geq \epsilon) = 0$*
4. *A càdlàg version.*

The future price process $(X_t)_{0 \leq t \leq T_2}$ in Definition 2.1 is here on the form

$$X_t = e^{Z_t} \tag{2.18}$$

where Z_t is an additive process, see Definition 2.14, such that X_t is a square integrable martingale. Let the spot price be modeled by

$$\log S_t = \Lambda_t + O_t + Y_t$$

where Λ_t is a deterministic seasonality function, O_t is an Ornstein-Uhlenbeck process $dO_t = \lambda O_t dt + dL_t^1$ and $dY_t = dL_t^2$. Set $L = (L^1, L^2)$ to be a two dimensional Lévy process and let L^1 and L^2 be independent on the probability space $(\Omega, \mathbb{P}, (\mathcal{F}_t)_{0 \leq t \leq T})$. Further, let Ψ_i be the cumulant function

for $L^i, i \in \{1, 2\}$ such that $E[e^{(z, L^1)}] = e^{\Psi(z)}$ for $z = (z_1, z_2) \in \mathbb{R}^2, |z| \leq C$. The independence of L^1 and L^2 gives $\Psi(z) = \Psi_1(z_1) + \Psi_2(z_2)$.

Benth and Detering (2014) present the Radon-Nokodym derivative:

$$\left. \frac{d\mathbb{Q}}{d\mathbb{P}} \right|_{\mathcal{F}_t} = \exp\{\theta^T L_t - t\Psi(\theta)\}.$$

The cumulant function under the risk neutral measure \mathbb{Q} is $\Psi^\theta(z) = \Psi(z + \theta) - \Psi(\theta)$. Under \mathbb{Q} the futures contract with delivery time between T_1 and T_2 is

$$F(t, T_1, T_2) = E^{\mathbb{Q}} \left[\frac{1}{T_2 - T_1} \int_{T_1}^{T_2} S_r dr | \mathcal{F}_t \right]$$

Let $F(t, T)$ be the artificial futures price for delivery at a single point in time, i.e. $F(t, T) = E[S_T | \mathcal{F}_t]$. We then have

$$F(t, T_1, T_2) = \frac{1}{T_2 - T_1} \int_{T_1}^{T_2} F(t, T) dT. \quad (2.19)$$

Proposition 2.15 *The artificial future price process $F(t, T)$ follows an exponential additive model under \mathbb{Q} given by*

$$F(t, T) = \tilde{h}_1(T) \tilde{h}_2(T - t) \exp\left\{ \tilde{L}_t^2 + e^{-\lambda T} \int_0^t e^{\lambda u} d\tilde{L}_u^1 \right\}, \quad t \leq T$$

where

$$\begin{aligned} \tilde{h}_1(T) &= \exp\left\{ \Lambda_T + O_0 e^{-\lambda T} + Y_0 + \frac{\partial \Psi_1^\theta(0)}{\lambda} (1 - e^{-\lambda T}) + \frac{\partial}{\partial z} \Psi_2^\theta(0) T \right\} \\ \tilde{h}_2(\tau) &= \exp\left\{ \tau \tilde{\Psi}_2^\theta(1) + \int_0^\tau \tilde{\Psi}_1^\theta(e^{-\lambda u}) du \right\} \end{aligned}$$

and \tilde{L}^i is defined by $\tilde{L}_t^i := L_t^i - \frac{\partial}{\partial z} \Psi_i^\theta(0) t$ and $\tilde{\Psi}_i^\theta(z) := \Psi_i^\theta(z) - \frac{\partial}{\partial z} \Psi_i^\theta(0) z$.

Proof. See Proposition 5.1 in Benth and Detering (2014). \square

We are however not interested in $F(t, T)$ but in $F(t, T_1, T_2)$. Using Proposition 2.15 and Equation (2.19) we get

$$F(t, T_1, T_2) = \frac{1}{T_2 - T_1} \int_{T_1}^{T_2} h_1(T) h_2(T - t) \exp\left\{ L_t^2 + e^{-\lambda T} \int_0^t e^{\lambda u} dL_u^1 \right\} dT$$

for $t < T_1$ where \tilde{h}_1 and \tilde{h}_2 have been replaced by the deterministic h_1 and h_2 , defined as \tilde{h}_i but with \tilde{L}^i and $\tilde{\Psi}_i^\theta$ replaced by L^i and Ψ_i^θ , respectively, and $\frac{\partial}{\partial z} \Psi_i^\theta(0) = 0$ for $i \in \{1, 2\}$, i.e.

$$\begin{aligned}
h_1(T) &= \exp\{\Lambda_T + O_0 e^{-\lambda T} + Y_0\}, \\
h_2(\tau) &= \exp\left\{\tau \Psi_2^\theta(1) + \int_0^\tau \Psi_2^\theta(e^{-\lambda u}) du\right\}.
\end{aligned}$$

However, the process $F(t, T_1, T_2)$ is not exponential additive due to T -dependency in the scaling of the L^1 integral. Because of that we want to find scaling terms $\Sigma^{T_1, T_2}(t) = (\Sigma_1(t), \Sigma_2(t))$ such that

$$\begin{aligned}
&F(t, T_1, T_2) \\
&\approx F(0, T_1, T_2) \exp\left\{-\int_0^t \Psi^\theta((\Sigma_1(s), \Sigma_2(s))) ds + \int_0^t \Sigma^{T_1, T_2}(s) dL_s\right\}.
\end{aligned} \tag{2.20}$$

Let $\hat{F}(t, T_1, T_2)$ be the approximation of Equation (2.20). We have

$$\hat{F}(0, T_1, T_2) = \frac{1}{T_2 - T_1} \int_{T_1}^{T_2} h_1(T) h_2(T) dT.$$

To obtain $\Sigma^{T_1, T_2}(t)$ we start with calculating the second moment of $F(t, T_1, T_2)$.

$$\begin{aligned}
&E^{\mathbb{Q}}\left[\frac{1}{(T_2 - T_1)^2} \left(\int_{T_1}^{T_2} F(t, T) dT\right)^2\right] \\
&= \frac{2}{(T_2 - T_1)^2} \int_{T_1}^{T_2} \int_{T_1}^u E^{\mathbb{Q}}[F(t, u) F(t, T)] dT du \\
&= \frac{2}{(T_2 - T_1)^2} \int_{T_1}^{T_2} \int_{T_1}^u S_0^2 h_1(u) h_1(T) e^{h(t, u, T)} dT du
\end{aligned} \tag{2.21}$$

where $h(t, u, T)$ is

$$h(t, u, T) = \int_0^t \Psi^\theta(e^{\lambda(s-u)} + e^{\lambda(s-T)}, 2) ds + \int_t^u \Psi^\theta(e^{\lambda(s-u)}, 1) ds + \int_t^T \Psi^\theta(e^{\lambda(s-T)}, 1) ds.$$

Then, we calculate the second moment of $\hat{F}(t, T_1, T_2)$

$$E^{\mathbb{Q}}[\hat{F}(t, T_1, T_2)^2] = \hat{F}(0, T_1, T_2)^2 e^{-2 \int_0^t \Psi^\theta(\Sigma^{T_1, T_2}(s)) ds + \int_0^t \Psi^\theta(2\Sigma^{T_1, T_2}(s)) ds}. \tag{2.22}$$

Finally, to get an expression for $\Sigma^{T_1, T_2}(t)$ set Equation (2.21) equal to Equation (2.22). If we take the logarithm and differentiating with respect to t we get

$$-2\Psi^\theta(\Sigma^{T_1, T_2}(t)) + \Psi^\theta(2\Sigma^{T_1, T_2}(t)) = \frac{g\left(t, \frac{\partial h(t, u, T)}{\partial t}\right)}{g(t, 1)}$$

with $g(t, \gamma(t, u, T))$ defined as

$$g(t, \gamma(t, u, T)) := \frac{2}{(T_2 - T_1)^2} \int_{T_1}^{T_2} \int_{T_1}^u S_0^2 h_1(u) h_1(T) e^{h(t, u, T)} \gamma(t, u, T) dT du.$$

Let us choose $\Sigma_2(t) = 1$ (Benth and Detering, 2014), we will then get

$$-2\Psi_1^\theta(\Sigma_1(t)) + \Psi_1^\theta(2\Sigma_1(t)) = \frac{g\left(t, \frac{\partial h_1(t, u, T)}{\partial t}\right)}{g(t, 1)} \quad (2.23)$$

where both sides should be positive and with

$$\frac{\partial h_1(t, u, T)}{\partial t} := \Psi_1^\theta(e^{\lambda(t-u)} + e^{\lambda(t-T)}) - \Psi_1^\theta(e^{\lambda(t-u)}) - \Psi_1^\theta(e^{\lambda(t-T)}).$$

Benth and Detering (2014) suggest that a suitable approximation of the distribution of the Lévy processes L^i is Normal Inverse Gaussian (NIG) distribution. The cumulative transform for the NIG distribution is given by

$$\Psi_{NIG}(z) = \delta\left(\sqrt{\alpha^2 - \beta^2} - \sqrt{\alpha^2 - (\beta + z)^2}\right) + \mu z.$$

We have that $\Psi_{NIG}(z)$ is strictly super additive, i.e. $\Psi_{NIG}(x+y) > \Psi_{NIG}(x) + \Psi_{NIG}(y)$ for $x, y \in \mathbb{R}, x+y \leq \alpha - \beta$ and that $\Psi_{NIG}(2z) - 2\Psi_{NIG}(z)$ is strictly increasing for $z \in \mathbb{R}, z \leq (\alpha - \beta)/2$, see Benth and Detering (2014). This gives a unique choice of $\Sigma_1(t)$ satisfying Equation (2.23).

Weron (2008) suggests that the spot price has a annual sinusoid cycle with a linear trend and Benth and Detering (2014) propose that the seasonality function can be estimated by

$$\Lambda_t = b_1 + b_2 \sin[2\pi(t/365 - b_3)] + b_4 t.$$

2.4.2 Option pricing

To derive an integral representation of the prices of call and put options under the process (2.18) we use $L_1(z)$ in Lemma 2.9.

Proposition 2.16 *The prices of call and put option at time t with payoff*

$C(X_{T_2}) = (X_{T_2} - K)^+$ and $P(X_{T_2}) = (K - X_{T_2})^+$, respectively, are

$$C(t, T_1, T_2) := E\left[(X_{T_2} - K)^+ | \mathcal{F}_t\right] = \frac{1}{2\pi i} \int_{c-i\infty}^{c+i\infty} e^{\int_t^{T_2} \Psi_s(z) ds} X_t^z \frac{K^{1-z}}{z(z-1)} dz$$

for $\Re(c) > 1$, $c \in \mathcal{D}$

$$P(t, T_1, T_2) := E\left[(K - X_{T_2})^+ | \mathcal{F}_t\right] = \frac{1}{2\pi i} \int_{c-i\infty}^{c+i\infty} e^{\int_t^{T_2} \Psi_s(z) ds} X_t^z \frac{K^{1-z}}{z(z-1)} dz$$

for $\Re(c) < 0$, $c \in \mathcal{D}$

(2.24)

where $\Psi_t(z)$ is defined according to Definition 2.18 below, $d\rho_t := d\Psi_t(z)$, \mathcal{D} is the set $z \in \mathcal{S}$ such that $\int_0^T \left| \frac{d\Psi_u(z)}{d\rho_u} \right| d\rho_u < \infty$ and assume that the interval $z \in \mathcal{C}$, $-2 < \Re(z) < 2$ is included in \mathcal{D} .

Proof. See Benth and Detering (2014) Section 3.3 and Goutte et al. (2014) Theorem 4.1. \square

Remark 2.17 Recall that a European option on the future price process X_t will have the same payoff as an Asian option on the spot price S_t . Due to the no arbitrage assumption, two different options with the same payoff must have same price. See Definition 2.2.

Definition 2.18 Let Z_t be an additive process according to Definition 2.14. The characteristic function $\phi(z) = E[e^{zZ_t}]$ for $z = ix$, $x \in \mathbb{R}$ is

$$\begin{aligned} \phi(z) &= E[e^{zZ_t}] = e^{\Psi_t(z)} \\ \Psi_t(z) &= \frac{1}{2} z^2 A_t + z \Gamma_t + \int_{[0,1] \times \mathbb{R}} (e^{zx} - 1 - zx \mathbb{1}_{|x| \leq 1}) \mu(ds, dx) \end{aligned}$$

for z with $\Re(z) \in \mathcal{S} := \{c \in \mathbb{R} | \int_{[0,T] \times \{|x| > 1\}} e^{cx} \mu(dt, dx) < \infty\}$ where A_t and Γ_t are constants and $\mu(t, B)$ is given by the unique measure integrating $1 \wedge |x|^2$ of the Lévy-Khinchin representation for the infinitely divisible distribution of Z_t .

2.4.3 Quadratic hedge

We want to determine the initial capital, the continuous hedging positions and the hedging position at time T_1 for the hedging portfolio V_t in Definition 2.3. The initial capital V_0 is given by the price of the option at time 0. The continuous hedging positions are given by the Proposition below.

Proposition 2.19 The positions for the hedging portfolio V_t at time $t < T_1$ for a call and put option, respectively, are given by

$$\begin{aligned}
\psi_t^{call} &= \frac{1}{2\pi i} \int_{c-i\infty}^{c+i\infty} \frac{d\rho_t(z, 1)}{d\rho_t} e^{\int_t^{T_2} \Psi_s(z) ds} X_{t-}^{z-1} \frac{K^{1-z}}{z(z-1)} dz \\
&\text{for } \Re(c) > 1, c \in \mathcal{D} \\
\psi_t^{put} &= \frac{1}{2\pi i} \int_{c-i\infty}^{c+i\infty} \frac{d\rho_t(z, 1)}{d\rho_t} e^{\int_t^{T_2} \Psi_s(z) ds} X_{t-}^{z-1} \frac{K^{1-z}}{z(z-1)} dz \\
&\text{for } \Re(c) < 0, c \in \mathcal{D}
\end{aligned} \tag{2.25}$$

with $d\rho_t(z, y) := d(\Psi_t(z+y) - \Psi_t(z) - \Psi_t(y))$.

Proof. See Benth and Detering (2014) Section 3.3. \square

The hedging position at time T_1 is given by the Proposition below.

Proposition 2.20 *The hedging position ψ_{T_1} for the portfolio V_t is given by*

$$\psi_{T_1} = \frac{\frac{1}{2\pi i} \int_{c-i\infty}^{c+i\infty} \mathcal{L}\{g(y)\}(z) e^{\Psi_{T_2}(z) - \Psi_{T_1}(z)} dz}{X_{T_1}^2 (e^{\Psi_{T_2}(2) - \Psi_{T_1}(2)} - 1)} \tag{2.26}$$

If we let $f(X_{T_1} e^y)$ be the payoff of a call or a put option, according to Lemma 2.9 we have

$$\mathcal{L}\{g(y)\}(z) = -\frac{X_{T_1}^2}{2-z} \left(\frac{K}{X_{T_1}}\right)^{2-z} + \frac{KX_{T_1} + X_{T_1}^2}{1-z} \left(\frac{K}{X_{T_1}}\right)^{1-z} + \frac{KX_{T_1}}{z} \left(\frac{K}{X_{T_1}}\right)^{-z}$$

for z with $\Re(z) > 2$ for call options and $\Re(z) < -2$ for put options .

Proof. See Benth and Detering (2014) Section 3.3. \square

2.5 Evaluation of models

To evaluate the hedging strategies we investigate the tracking error and the hedging error of the models. Both the tracking error and the hedging error are defined as the difference of the hedging portfolio and the payoff of the option at time T_2

$$V_{T_2} - \left(\frac{1}{T_2 - T_1} \int_{T_1}^{T_2} S_r dr - K \right)^+ \tag{2.27}$$

where $\left(\frac{1}{T_2 - T_1} \int_{T_1}^{T_2} S_r dr - K \right)^+$ is the payoff of the Asian call option at time T_2 and V_{T_2} is the hedging portfolio at time T_2 . The difference between the tracking error and the hedging error is that the tracking error bases the

payoff of the option on historical data and shows thus how the hedge would have performed historically if used. The hedging error simulates the entire price process, including the final payoff of the option. The advantage is that it is possible to investigate more outcomes for the payoff of the option than when investigating the tracking error. However, the result from the hedging error will only be relevant if the future price process X_t follows the actual future price process correctly.

Chapter 3

Simulation of electricity futures prices

The two first models in the theory section, the geometric Brownian motion model and the stochastic volatility model, are tested empirically. This chapter presents methods for estimating the parameters for each of the two models along with simulation techniques. Furthermore, the chapter begins with a data analysis of the spot prices and futures contracts in the data sample.

3.1 Data analysis

In Figure 3.1 and 3.2 we can see the daily average of spot base load electricity prices between 2006 and 2014 and the daily average of futures prices for a one month contract¹ on base load electricity prices between 2010 and 2014, respectively. The spot price data is collected from Nord Pool and the futures price data is collected from Bloomberg. Because of the change in composition in 2006 of hydro, nuclear, wind and water power, leading to higher volatility, the data from before 2006 is not relevant for the current spot price. In total, there are 3217 observations of the spot price and 3643 observations of the futures prices. All prices are denoted in EUR per MWh. There are prices for three months for each futures contract, i.e. around 60 data points for each contract. The delivery period is the month after the last trading day, or more precisely, the May contract's delivery period is May but its last trading day is the last of April (or the last trading day in April).

From a visual inspection we can see in Figure 3.1 and 3.2 that the spot price is more volatile than the futures price, as expected. The spot price shows both seasonality and spiky behavior. The futures price appears to show some seasonality as well, but it is not as evident as the for spot price.

¹A one month futures contract means that its delivery period is one month.

The futures prices have some spikes during the first two years, but after 2012 the prices are less spiky and have lower values. The spot prices also have more spikes during 2010-2012.

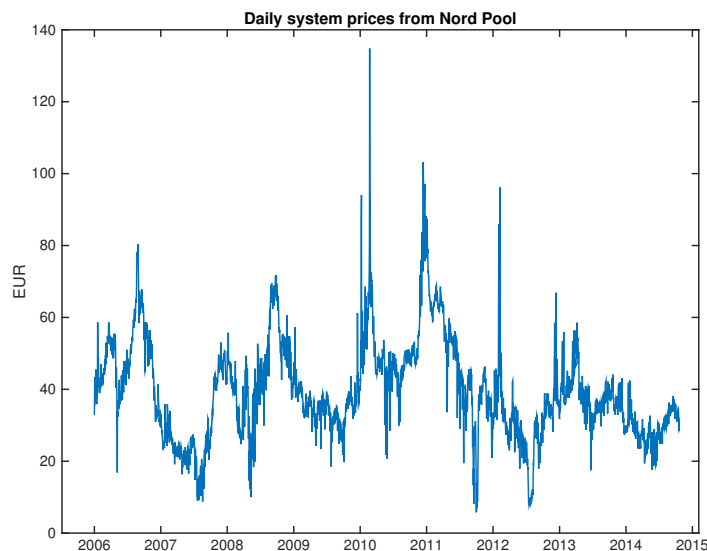


Figure 3.1: Daily spot prices of system prices from Nord Pool
2006-02-01 - 2014-10-22

Table 3.1 shows the average, minimum, maximum and standard deviation for futures prices. To detect seasonal differences, there are also the same statistics month-wise. Note that the volatility is annualized by multiplying the daily standard deviation by $\sqrt{250}$, since 250 is the average number of trading days per year. In the sample, April has the highest volatility and November the lowest. The highest values of the futures contracts can be found in January to Mars and the lowest in July and August. The standard deviation is the highest in the beginning of the year and the lowest in the end. Note that the volatilities for 2010-2012 are approximately the same but that it drops significantly in 2013 and 2014. We can see that the prices are lower during the last two years as well.

3.2 Geometric Brownian motion

3.2.1 Estimation of α and $\hat{\sigma}$

Recall that $\log(X_t/X_s) \sim N(-\frac{1}{2}\tilde{\sigma}_{s,t}^2, \tilde{\sigma}_{s,t}^2)$, we can then use Maximum Likelihood estimation to fit the empirical log returns to that normal distribution with time dependent parameters. The probability density function of

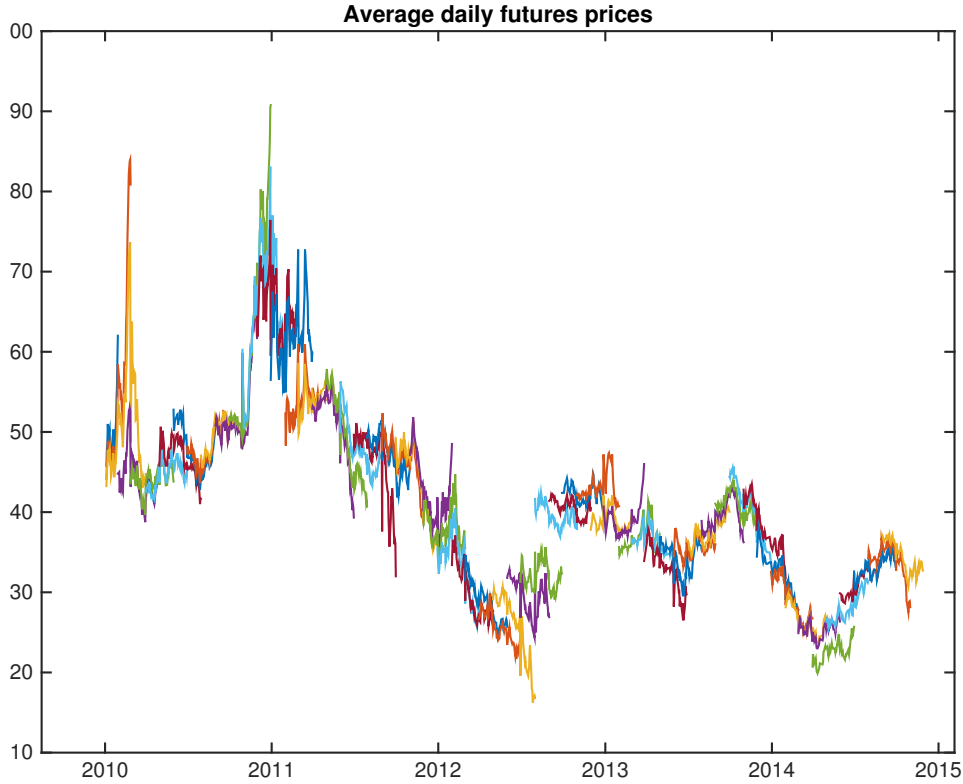


Figure 3.2: Futures contracts with one month delivery. 3 months data for each contract. Data from Bloomberg
2010-02-01 - 2014-11-28

$\log(X_{t+1}/X_t)$ is given by

$$f(x) = \frac{1}{\sqrt{2\pi}\tilde{\sigma}_{t,t+1}} \exp\left\{-\frac{(x + \frac{1}{2}\tilde{\sigma}_{t,t+1}^2)^2}{2\tilde{\sigma}_{t,t+1}^2}\right\} \quad (3.1)$$

where $\tilde{\sigma}_{t,t+1}^2$ is as in Equation (2.3) and $x = \log(X_{t+1}/X_t)$. Matlab's function `mle` is used with (3.1) and empirical data. Since the volatility depends on time to maturity, contract-wise estimation of the parameters is done. The futures contracts seem to be showing some seasonality, see Figure 3.2 and Table 3.1, therefore the estimation of parameters for the 2014 futures contracts is done on data for the equivalent month in 2013. There are three months data for each contract, i.e. around 60 data points per contract. The estimations along with a 95% confidence interval are presented in Table 3.2. The last row is for all front month contracts 2010-2013, 989 data points, as

	Mean	Min	Max	St. dev.	# Obs	Volatility	# Obs
Total	41.06	16.25	90.77	10.82	3702	23.72%	3643
January	47.38	33.70	90.77	11.11	252	21.66%	248
February	47.69	31.75	83.10	11.31	275	29.20%	270
Mars	45.52	27.60	83.95	13.63	289	27.73%	284
April	42.97	25.25	73.70	13.09	316	32.16%	311
May	38.36	27.70	60.95	10.19	309	23.14%	304
June	37.97	23.00	58.50	10.69	309	18.56%	304
July	35.38	19.90	56.00	11.26	304	21.50%	299
August	36.75	16.25	57.85	10.16	320	27.86%	315
September	38.45	24.35	56.30	8.28	330	23.13%	325
October	39.43	29.10	52.60	7.14	334	24.00%	329
November	42.00	27.50	52.50	6.12	334	13.96%	329
December	43.02	30.75	68.33	6.80	330	16.78%	325
2010	51.10	38.75	90.77	9.06	765	27.89%	761
2011	50.61	32.00	77.00	7.61	759	26.08%	757
2012	33.96	16.25	48.50	6.52	753	27.44%	751
2013	37.75	26.50	47.40	3.33	747	16.63%	754
2014	30.54	19.90	37.55	4.21	750	16.45%	629

Table 3.1: Statistics of the futures contracts with one month delivery 2010-2014. 3702 observations in total. Note that the volatility corresponds to the annualized standard deviation of the log-return. The number of observations for the log-return is 3643.

comparison. Figure 3.3 shows the empirical distribution density along with the estimated time dependent normal density for log returns of the JUL 13 contract.

We can see that the empirical distribution has heavier tails and an expected value closer to zero than the fitted normal distribution. This indicates that the normal distribution is a bad fit for electricity futures log returns, despite the adjustment with time dependent volatility. Another indication of a bad fit of the distribution is the rather large confidence intervals for α and $\hat{\sigma}$ along with the fact that the estimation of α is zero for several months, and that the confidence interval includes zero in some additional months. The estimation for the APR 13 contract was not possible to derive. In these cases, when the estimation of α is inadequate, parameters for a month close by is used in the simulation of the hedge. Both α and $\hat{\sigma}$ varies significantly between the months, this might be because of the seasonal variations, or just due to large differences between each contract.

	α		$\hat{\sigma}$	
JAN13	2.062	(0.918, 3.207)	0.034	(0.013, 0.054)
FEB13	4.242	(2.241, 6.063)	0.011	(-0.002, 0.024)
MAR13	0.000	(-2.163, 2.163)	0.099	(0.051, 0.147)
APR13	-		-	
MAY13	2.849	(1.535, 4.163)	0.027	(0.006, 0.048)
JUN13	0.000	(-1.931, 1.931)	0.100	(0.051, 0.149)
JUL13	1.327	(0.061, 2.593)	0.079	(0.032, 0.126)
AUG13	0.000	(-1.744, 1.744)	0.121	(0.069, 0.173)
SEP13	0.000	(-1.103, 1.103)	0.096	(0.073, 0.119)
OCT13	0.770	(-0.424, 1.963)	0.070	(0.038, 0.102)
NOV13	0.000	(-1.186, 1.186)	0.084	(0.058, 0.109)
DEC13	1.224	(-0.005, 2.453)	0.055	(0.025, 0.085)
FRONT	0.000	(-0.573, 0.573)	0.128	(0.106, 0.149)

Table 3.2: The estimation of $\hat{\sigma}$ and α is for futures contracts with one month delivery. Data used is three month of each 2013 contract and front month contracts 2010-1013. A 95% confidence interval is provided in parenthesis.

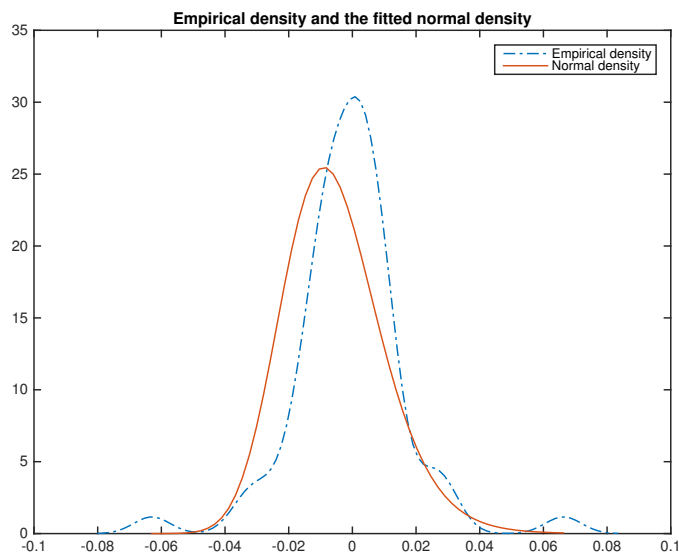


Figure 3.3: Empirical probability density and fitted normal density with time dependent parameters for the log return of JUL13.

3.2.2 Simulation

Wiener process

From the distribution of $\log(X_t/X_s)$ we can write

$$\log X_{t+1} = \log X_t - \frac{1}{2}\tilde{\sigma}_{t,t+1}^2 + \tilde{\sigma}_{t,t+1}Z_t$$

where $\tilde{\sigma}_{t,t+1}^2$ is defined in (2.3) and Z_t is i.i.d. standard normally distributed random variables. Figure 3.4 presents 10 sample paths of the geometric Brownian motion X_t with $\alpha = 2.062$, $\hat{\sigma} = 0.034$ and initial value 39.30 EUR.

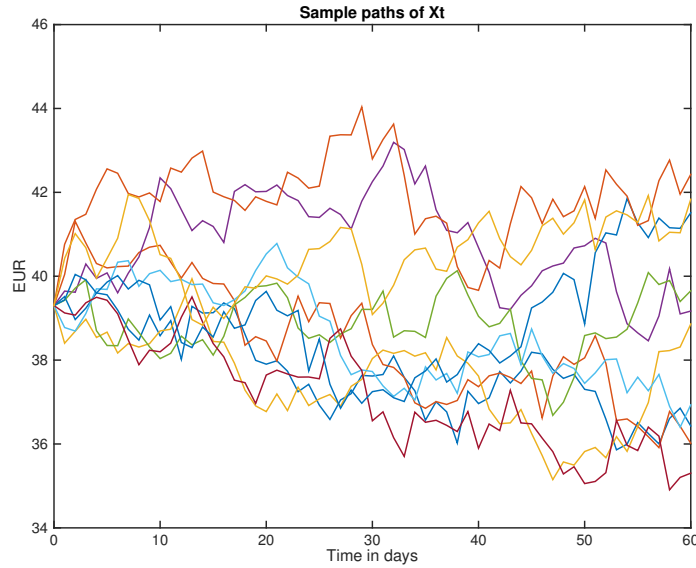


Figure 3.4: 10 sample paths of X_t with $\alpha = 2.062$, $\hat{\sigma} = 0.034$ and initial value 39.30 EUR.

Hedging portfolio

The hedge is rebalanced on a daily basis. The integral in Definition 2.3 will then be estimated by the sum

$$V_t \approx V_0 + \sum_{k=1}^n \psi_t(X_{t_k} - X_{t_{k-1}}) + \mathbb{1}_{t > T_1} \psi_{T_1}$$

with $t_n = t$ and $t_k - t_{k-1} = 1$. The option is issued two months before delivery on a one month futures contract, i.e. we start at time 0 and $T_1 = 60$ and $T_2 = 90$.

3.3 Stochastic volatility

3.3.1 Estimation of parameters

The method for estimating the parameters for the stochastic volatility model is based on the method in Benth (2011), where we start with a linear regression and fit its residuals to the autocorrelation function of the future price process. Subsequently, the residuals' distribution is approximated with a suitable distribution. Here the data used for estimation of parameters is the historical prices for the front month futures contract on base load electricity prices 2010-2013 with 989 observations. The dynamics of the log prices Z_t give

$$Z_{t+1} = Z_t - \frac{1}{2} \int_t^{t+1} \sigma_s^2 ds + \int_t^{t+1} \sigma_s dB_s,$$

i.e. a linear regression of tomorrow's log prices. Since Z_t is a martingale, its expected value is its previous value and the remaining part of the expression is its residual. Because of σ_t the residuals are probably not normally distributed. Figure 3.5 shows a scatterplot of Z_t against Z_{t+1} , which looks linear. The intercept of the regression is not significantly different from zero, to reduce it further incorporating a seasonality function in X_t , which then is subtracted from the data set, might be successful. The slope of the regression is 0.99, almost 1, with p-value 0, suggesting that the lack of mean reversion in the model for X_t is a reasonable estimate. The R^2 for the regression is 98%.

We now move on to investigate the residuals of the regression. Note that the residuals correspond to the the log returns of the futures prices X_t . The mean of the residuals is zero and the standard deviation 0.0162, which corresponds to a 25.69% yearly volatility (assuming 250 trading days per year). Barndorff-Nielsen and Shephard (2001) derive the variance and covariance for the log returns with stochastic volatility on the same form as in this model. Benth (2011) and Barndorff-Nielsen and Shephard (2001) suggest the *NIG* distribution as an approximate distribution of the residuals. Figure 3.7 shows the empirical density for the residuals, also suggesting that *NIG* might be a good distribution in our case. For *NIG* distributed residuals with $var(\sigma_t^2) = \omega^2$ we have that the covariance for the squared residuals y_t^2 is (see Barndorff-Nielsen and Shephard (2001), Section 5), for $s > 0$

$$\begin{aligned} cov(y_t^2, y_{t+s}) &= cov(\sigma_t^2, \sigma_{t+2}^2) \\ &= \omega^2 \lambda^{-2} (1 - exp\{-\lambda\})^2 exp\{-\lambda(s-1)\}, \end{aligned}$$

and the correlation is

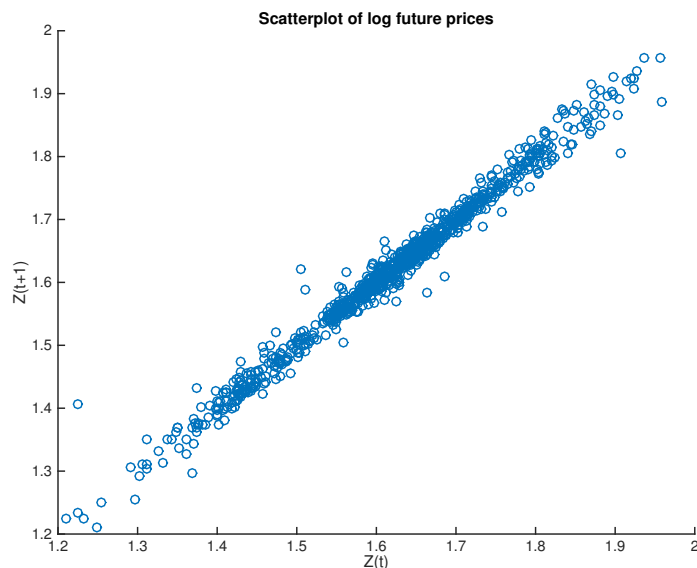


Figure 3.5: Scatterplot of futures log prices Z_t against Z_{t+1} for front month contracts 2010-2013.

$$\begin{aligned} \text{corr}(y_t^2, y_{t+s}^2) &= \text{corr}(\sigma_t^2, \sigma_{t+s}^2) \\ &= \lambda^{-2}(1 - \exp\{-\lambda\})^2 \exp\{-\lambda(s-1)\}. \end{aligned} \quad (3.2)$$

This allows us to fit the function in (3.2) to the autocorrelation function of the squared residuals. Figure 3.6 shows the autocorrelation function for the residuals together with the autocorrelation for the squared residuals with the fitted function (3.2). We can see that there is zero correlation since all of the lags are within the 95% interval around zero for the autocorrelation. Using nonlinear least squares we get an estimation of λ presented in Table 3.3 with an R^2 of 72%.

The empirical density² of the residuals is plotted in Figure 3.7 along with the *NIG* density with the fitted parameters in Table 3.3. Barndorff-Nielsen and Shephard (2001) showed that if the subordinator process L_t has *IG*(α, δ) distributed marginals, then residuals will be *NIG*($\alpha, 0, 0, \delta$) distributed (given that the mean and the skewness of the residuals are zero). The parameters to the *NIG* distribution are estimated using Maximum Likelihood and presented in Table 3.3. However, the confidence intervals are rather large, especially for α . Inspection of Figure 3.7 indicates that the fitted distribution is slightly more peaky but otherwise a good fit.

²using Matlab's function `ksdensity`

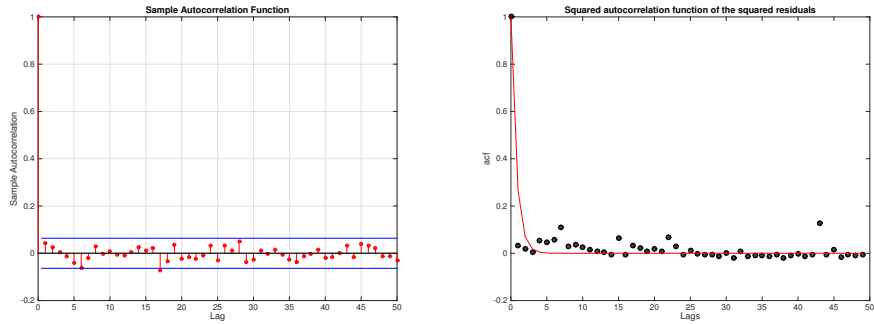


Figure 3.6: Autocorrelation of the residuals and the squared autocorrelation of the residuals together with a fitted curve $\lambda^{-2}(1 - \exp\{-\lambda\})^2 \exp\{-\lambda(s - 1)\}$, $\lambda = 1.335$ for the 50 first lags.

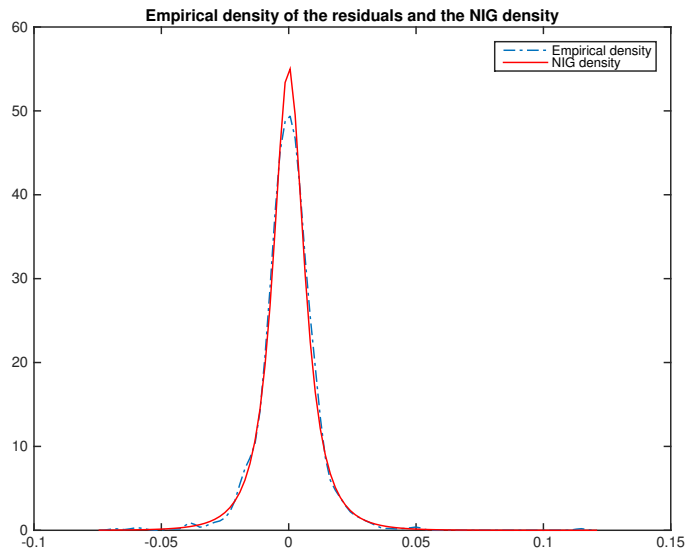


Figure 3.7: Empirical density of the residuals and the *NIG* density with parameters $\alpha = 41.53$, $\beta = 0$, $\mu = 0$ and $\delta = 0.010$.

	Estimate	95% Confidence interval
α	41.53	(31.00, 52.07)
δ	0.010	(0.0086, 0.0113)
λ	1.335	(1.317, 1.352)

Table 3.3: Parameter estimation for the stochastic volatility model.

3.3.2 Simulation

Stochastic processes

For the stochastic volatility model there are several stochastic processes to be simulated; the stochastic volatility driven by a Lévy process and the future price process driven by a Wiener process. The stochastic processes that drive the volatility and future price process are on integral form. A stochastic integral can be estimated by the Riemann sum

$$\int_t^T f(s) dY_s \approx \sum_{k=1}^n f(t_k)(Y_{t_{k+1}} - Y_{t_k})$$

with $t_k = k\Delta t$.

If we choose L_t to be an inverse Gaussian process we have that $L_1 \sim IG(\delta, \gamma)$. The cumulant function of the IG process (see Equation (2.14)) implies that $L_t \sim IG(t\delta, \gamma)$. Since the IG process is a Lévy process it has independent increment and is stationary. This together with the distribution of L_t give $L_{t+s} - L_t \sim IG(s\delta, \gamma)$ with $L_0 = 0$ and $L_t = \sum_{k=1}^{\lfloor t/\tau \rfloor} \tilde{L}_{t_k}$ where $\tilde{L}_{t_k} \sim IG(\tau\delta, \gamma)$ i.i.d. random variables and τ the time interval. In Figure 3.8 we can see one realization of the process L_t . The process displays an upward trend with some large jumps. Using this, modeling the stochastic volatility σ_t^2 (2.8) can be done by

$$\begin{aligned} \sigma_t^2 &\stackrel{d}{\approx} \sigma_s^2 e^{\lambda(t-s)} + \sum_{k=1}^n e^{\lambda(t_{k+1}-t)} (L_{k+1} - L_k) \\ &\stackrel{d}{=} \sigma_s^2 e^{\lambda(t-s)} + \sum_{k=0}^n e^{\lambda(t_{k+1}-t)} \tilde{L}_k \end{aligned}$$

with and $\tilde{L}_{t_k} \sim IG((t_{k+1} - t_k)\delta, \gamma)$ i.i.d. random variables. Similarly, the first part of the log prices (2.12) can be modeled as,

$$\begin{aligned} -\frac{1}{2} \int_s^t \sigma_u^2 du &= -\frac{1}{2} \left(\sigma_s^2 \epsilon(s, t) + \int_s^t \epsilon(u, t) dL_u \right) \\ &\stackrel{d}{\approx} -\frac{1}{2} \left(\sigma_s^2 \epsilon(s, t) + \sum_{k=1}^n \epsilon(t_k, t) \tilde{L}_k \right) \end{aligned}$$

with $\tilde{L}_{t_k} \sim IG((t_k - t_{k-1})\delta, \gamma)$ i.i.d. random variables.

For a Wiener process B_t with $B_1 \sim N(0, 1)$ we have that marginally $B_t \sim N(0, t)$ with independent increments $B_{t+s} - B_t \sim N(0, s)$ (Barndorff-Nielsen and Shephard, 2012). We can therefore simulate the remaining part of the log return as

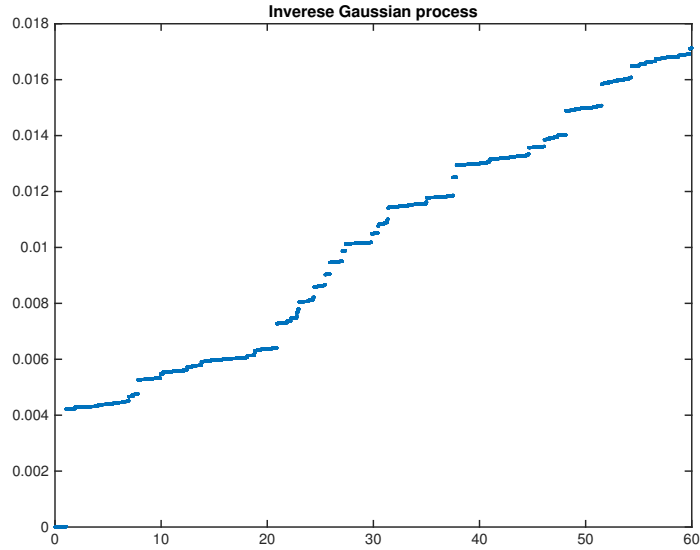


Figure 3.8: L_t as an inverse Gaussian process with parameters $\delta = 0.010$, $\gamma = 41.53$ and time interval $1/2000$.

$$\int_s^t \sigma_u dB_u \stackrel{d}{\approx} \sum_{k=1}^n \sigma_{t_k} (B_{k+1} - B_k) \stackrel{d}{=} \sum_{k=1}^n \sigma_{t_k} \sqrt{t_{k+1} - t_k} Z_k$$

with Z_k independent standard normally distributed random variables. Figure 3.9 shows 10 different sample paths of X_t .

Hedging portfolio

The hedge is rebalanced on a daily basis. The integral in Definition 2.3 will then be estimated by the sum

$$V_t \approx V_0 + \sum_{k=1}^n \psi_t(X_{t_k} - X_{t_{k-1}}) + \mathbb{1}_{t > T_1} \psi_{T_1}$$

with $t_n = t$ and $t_k - t_{k-1} = 1$. The option is issued two months before delivery on a one month futures contract, i.e. we start at time 0 and $T_1 = 60$ and $T_2 = 90$.

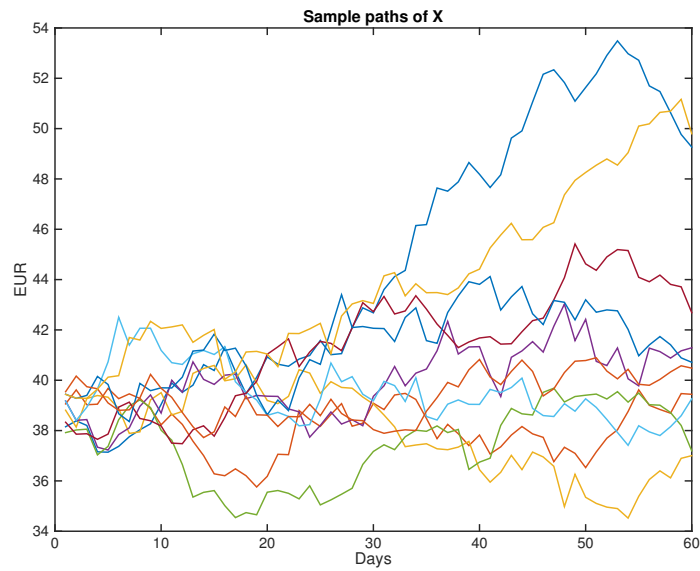


Figure 3.9: 10 sample paths of X_t with $X_0 = 39.30$, $\sigma_0 = 0.2569$, $\lambda = 1.335$, $\delta = 0.010$ and $\gamma = 41.53$.

Chapter 4

Results

The tracking error (based on historical data) and the hedging error (based on simulated values), see Equation (2.27), are presented to get a better view of the models' performance. While the tracking error shows how the models actually would have performed if used in 2014 the hedging error shows the performance for a larger number of outcomes. Given that the underlying model simulates the electricity futures accurately, the hedging error shows how the models would perform for more outcomes of the option's payoff than 2014 can provide. However, neither of the models are likely to exactly simulate the behavior of the electricity futures. The primary goal is though to investigate their performance in comparison to each other; if the more complex stochastic volatility model outperforms the simpler geometric Brownian motion. We will consider the tracking and hedging error for a call option using the geometric Brownian motion (GBM) and stochastic volatility (SV) model, respectively.

4.1 Hedging error

Figure 4.1 shows the simulated end values of the GBM model and the SV model, respectively, along with historical front month futures prices. Figure 4.2 presents the hedging error for the GBM and the SV model. The simulation is run 10,000 times with initial futures price 39.30 EUR and the same value of the strike price. Statistics for the simulations are shown in Table 4.1. The parameters used in the GBM model are those estimated on the JAN 13 contract.

We can see that the large negative values for the two models seem to be about the same. However, the SV model tends to overestimate the hedging portfolio resulting in an average around two instead of zero as in the GBM model. Table 4.1 shows that the value at risk is greater for the SV model, the median is however very similar. The spread between the minimum and maximum value for the GBM model is quite close to that of the SV model,

	Median	Min	Max	$VaR_{0.95}$	C_0
GBM	0.33	-9.02	3.08	2.57	0.16
SV	0.74	-11.40	2.08	3.60	1.82

Table 4.1: Statistics for hedging error for a call option with one month delivery for the geometric Brownian motion (GBM) model and stochastic volatility (SV) model, respectively. Strike price equal to the initial futures value 39.30 EUR and initial call price $C_0 = C(0, T_1, T_2)$. Starting hedge at time 0, 30 days prior to delivery, i.e. $T_1 = 30$ and $T_2 = 60$. Simulation run 10,000 times.

but slightly more narrow. Note that the SV model prices the option much higher than the GBM model. From the histograms in Figure 4.1 we can see that the SV model has heavier tails than the GBM model. Comparing with the empirical outcome of front month prices 2010-2013 shows even heavier tails than both the SV and the GBM model. Because of the heavier tails in the SV model the possible movement in the underlying asset is greater compared to the GBM model, which increases the hedging error.

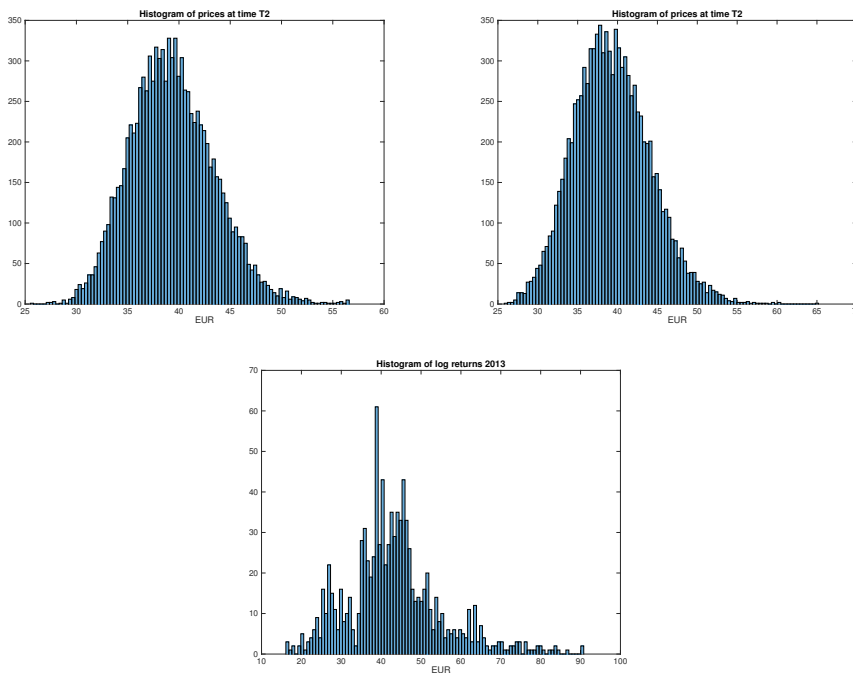


Figure 4.1: Histogram of prices at time T_2 , initial price 39.30. Simulation run 10,000 times. The geometric Brownian motion model in the upper left figure and the stochastic volatility model in the upper right, empirical values of the front month contracts in the lower.

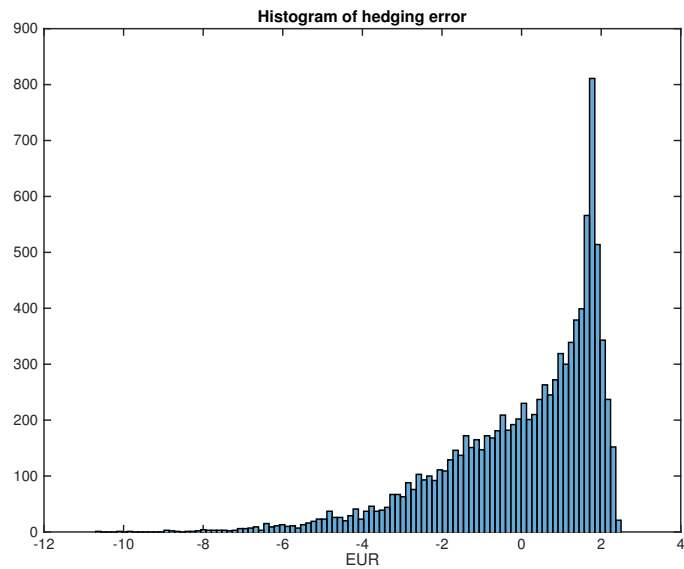
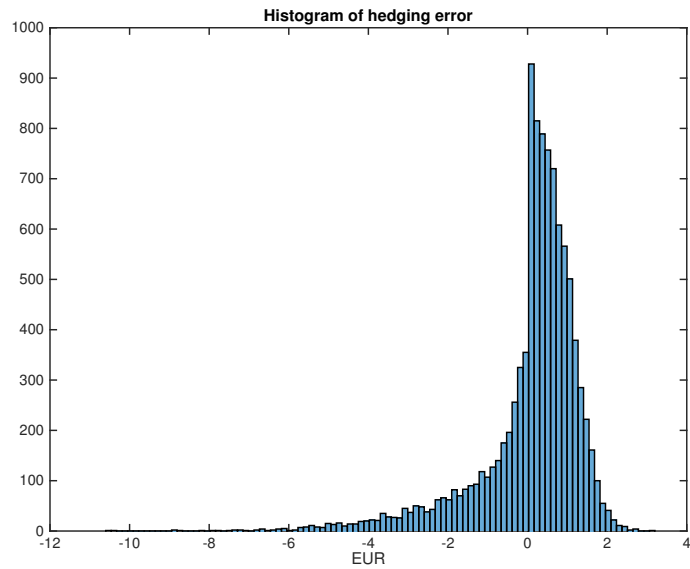


Figure 4.2: Histogram of hedging error for a call option with one month delivery, initial price 39.30 and strike price 39.30. Starting hedge at time 0, 30 days prior to delivery, i.e. $T_1 = 30$ and $T_2 = 60$. Simulation run 10,000 times. The geometric Brownian motion in the upper figure and the stochastic volatility in the lower.

4.2 Tracking error

Table 4.2 shows statistics for the tracking error when testing the GBM and the SV hedge, respectively, on 2014 data. The parameters used are estimated according to the methods described in Section 3.2 and 3.3. The estimation of α for the GBM model becomes 0 for some months, for these months the parameters of a close by contract are used, i.e. parameters from February are used in March, from May in April, from July in June, August and September, and from December in October and November. For the SV model, initial value of the volatility is set to be the yearly standard deviation of the residuals of the front month contracts 25.65%. Recall that positive values of the tracking error indicate that the portfolio value is greater than the claim, and negative values indicate the opposite. Worth noting is that the call option is only exercised in May, July, August and September, see the payoffs in the last column of Table 4.2.

While the values for the SV model are quite stable the result from the GBM model varies significantly between the months. This is not very surprising considering that the parameters are constant for all months in the SV model but different depending on month in the GBM model. The GBM model performs better in February to April in terms of closer spread between minimum and maximum values as well as smaller value at risk. Note that none of the options during these months are exercised. In May the option is exercised and the same parameters as in April are used in the GBM model. Here we can see that the median value is negative in the GBM model but positive in the SV model, value at risk is greater for the GBM model (but very similar to the corresponding SV value), but that spread is somewhat more narrow in the GBM model. This indicates that the GBM model for those parameters performs worse than the SV model when the price increases compared to the initial price. The subsequent months, June to September, all have the same parameters in the GBM model. Here the spread for the tracking error is much wider and the value at risk is greater than for the SV model. However, the median value is slightly better for the GBM model in July and August, when the price moved more than in the other months. Note that January is the month where the values in the GBM and SV model are most similar in terms of spread, value at risk and median value. Also here, the SV model performs better. In the last three months, when the parameters for the GBM model is estimated on the December contract, the SV model performs better as well. The SV model has smaller value at risk, tighter spreads of minimum and maximum value and smaller median values for these months.

2014	Median	Min	Max	$VaR_{0.95}$	C_0	F_0	F_{T_2}	$payoff$
<i>Geometric Brownian motion</i>								
Jan	1.00	-8.44	20.55	1.58	0.26	39.30	33.60	0.00
Feb	0.12	-1.61	2.95	0.35	0.05	35.30	30.23	0.00
Mar	0.11	-1.42	2.60	0.31	0.05	31.10	26.74	0.00
Apr	0.39	-3.89	8.29	0.77	0.12	27.00	25.52	0.00
May	-0.33	-4.39	7.17	1.42	0.11	25.60	26.30	0.70
Jun	2.09	-11.50	64.20	2.74	0.49	26.25	25.19	0.00
Jul	-3.78	-15.33	52.39	7.49	0.44	23.48	28.52	5.04
Aug	-1.47	-16.62	65.62	6.68	0.53	28.35	32.07	3.72
Sep	1.41	-16.04	81.16	4.78	0.63	33.70	34.97	1.27
Oct	3.09	-20.49	88.58	3.48	0.57	34.33	30.23	0.00
Nov	1.92	-15.05	45.29	2.54	0.35	34.60	30.19	0.00
Dec	1.81	-14.12	42.47	2.38	0.32	32.45	31.48	0.00
<i>Stochastic volatility</i>								
Jan	1.84	-7.92	15.60	0.97	1.82	39.30	33.60	0.00
Feb	1.66	-7.12	14.02	0.87	1.64	35.30	30.23	0.00
Mar	1.45	-6.27	12.35	0.77	1.44	31.10	26.74	0.00
Apr	1.27	-5.44	10.72	0.67	1.25	27.00	25.52	0.00
May	0.50	-5.86	9.47	1.33	1.87	25.60	26.30	0.70
Jun	1.23	-5.29	10.42	0.65	1.22	26.25	25.19	0.00
Jul	-3.92	-9.77	4.28	5.61	1.09	23.48	28.52	5.04
Aug	-2.39	-9.43	7.53	4.42	1.32	28.35	32.07	3.72
Sep	0.31	-8.06	12.11	2.10	1.56	33.70	34.97	1.27
Oct	1.56	-7.11	15.77	1.21	1.59	34.33	30.23	0.00
Nov	1.57	-7.17	15.89	1.22	1.61	34.60	30.19	0.00
Dec	1.47	-6.72	14.01	1.14	1.51	32.45	31.48	0.00

Table 4.2: Statistics for tracking error for a call option with one month delivery in January to September 2014. Strike price equal to the initial futures value $F_0 = F(0, T_1, T_2)$, initial call price $C_0 = C(0, T_1, T_2)$ and the final value of the futures contract $F_{T_2} = F(T_2, T_1, T_2)$. Starting hedge at time 0, 30 days prior to delivery, i.e. $T_1 = 30$ and $T_2 = 60$. Simulation run 10,000 times.

Chapter 5

Conclusion

This thesis empirically evaluates a geometric Brownian motion and a stochastic volatility model for modeling futures prices and hedging Asian call options on the electricity spot price. Estimation of parameters for the model is done based on historical futures contracts with a one month delivery period using nonlinear regression and Maximum Likelihood techniques. The models are tested on 2014 data and the tracking and hedging error for each model are presented. The tracking error is investigated through the median value, the spread between minimum and maximum value along with value at risk at a 95% level.

The stochastic volatility model performs better than the geometric Brownian motion, especially during the months where the arithmetic value of the spot price for the delivery month is higher than the initial futures price, i.e. when the option is exercised. The estimation of parameters for the geometric Brownian motion, done contract-wise for the 2013 contracts, produced several inadequate estimations, where the confidence interval of one the parameters included zero. This indicates that the log returns of electricity futures are not normally distributed with time dependent volatility. The estimation of parameters for the different months produced significantly different tracking errors. Although some seasonality could be detected in the historical futures prices, the results do not show any benefits from estimating parameters based on month.

An implication when using historical futures prices for estimation of parameters is that the prices are not continuous from contract to contract. The estimation can therefore either be based on data from one contract, which only provides a very limited amount of data points, or (incorrectly) assume that the front month contracts are continuous and from the same time series. The latter approach provides more data points and uses liquid contracts, as opposed to the former approach where many contracts suffer from illiquidity before the front month.

The year 2014 had quite low and stable prices compared to earlier years,

the result would probably have been very different if tested on a more volatile year. Considering that the worst months for the tracking error are when the prices moved the most, the models would perform worse for such a year.

The performance might be improved by adding seasonality to the models. For the stochastic volatility model, the mean reverting factor could be time dependent or a drift term depending on the season could be added.

In conclusion, the more complex stochastic volatility model performs better in general compared to the geometric Brownian motion when it comes to tracking error for 2014 data. In addition, it also provides more satisfactory estimates of parameters and a better fit of the distributions of log returns.

Bibliography

- Aïd, R., Campi, L., and Langrené, N. (2013). A structural risk-neutral model for pricing and hedging power derivatives. *Mathematical Finance*, 23(3):387–438.
- Barndorff-Nielsen, O. E. (1997). Processes of normal inverse gaussian type. *Finance and stochastics*, 2(1):41–68.
- Barndorff-Nielsen, O. E. and Shephard, N. (2001). Non-gaussian ornstein–uhlenbeck-based models and some of their uses in financial economics. *Journal of the Royal Statistical Society: Series B (Statistical Methodology)*, 63(2):167–241.
- Barndorff-Nielsen, O. E. and Shephard, N. (2012). Basics of lévy processes. *Draft Chapter from a book by the authors on Lévy Driven Volatility Models*.
- Benth, F. E. (2011). The stochastic volatility model of barndorff-nielsen and shephard in commodity markets. *Mathematical Finance*, 21(4):595–625.
- Benth, F. E. and Detering, N. (2014). Pricing and hedging asian-style options in energy. *Working paper, Available at SSRN 2330273*.
- Bierbrauer, M., Menn, C., Rachev, S. T., and Trück, S. (2007). Spot and derivative pricing in the eex power market. *Journal of Banking & Finance*, 31(11):3462–3485.
- Eberlein, E. and Raible, S. (1999). Term structure models driven by general lévy processes. *Mathematical Finance*, 9(1):31–53.
- Forsell, M. (2015). Trader at SEB Commodities. Interview 2015-02-20.
- Goutte, S., Oudjane, N., and Russo, F. (2014). Variance optimal hedging for continuous time additive processes and applications. *Stochastics An International Journal of Probability and Stochastic Processes*, 86(1):147–185.
- Heppenger, P. (2012). Hedging electricity swaptions using partial integro-differential equations. *Stochastic Processes and their Applications*, 122(2):600–622.

- Hinz, J., Von Grafenstein, L., Verschuere, M., and Wilhelm, M. (2005). Pricing electricity risk by interest rate methods. *quantitative finance*, 5(1):49–60.
- Jean-Pierre, F., Papanicolaou, G., and Sircar, K. R. (2000). *Derivatives in financial markets with stochastic volatility*. Cambridge University Press.
- Lucia, J. J. and Schwartz, E. S. (2002). Electricity prices and power derivatives: Evidence from the nordic power exchange. *Review of Derivatives Research*, 5(1):5–50.
- NASDAQOMX (2015). Contract specifications - commodity derivatives. http://www.nasdaqomx.com/digitalAssets/97/97180_150202-joint-appendix-2---contract-specifications.pdf. [Online; accessed 2015-02-10].
- Nicolato, E. and Venardos, E. (2003). Option pricing in stochastic volatility models of the ornstein-uhlenbeck type. *Mathematical finance*, 13(4):445–466.
- NordPool (2015). Nord pool spot. <http://www.nordpoolspot.com/#/nordic/table>.
- Samuelson, P. A. (1965). Proof that properly anticipated prices fluctuate randomly. *Industrial management review*, 6(2):41–49.
- Vehvilainen, I. (2002). Basics of electricity derivative pricing in competitive markets. *Applied Mathematical Finance*, 9(1):45–60.
- Weron, R. (2008). Market price of risk implied by asian-style electricity options and futures. *Energy Economics*, 30(3):1098–1115.
- Weron, R., Simonsen, I., and Wilman, P. (2004). Modeling highly volatile and seasonal markets: evidence from the nord pool electricity market. In *The application of econophysics*, pages 182–191. Springer.